

ISTANBUL TECHNICAL UNIVERSITY ★ GRADUATE SCHOOL OF SCIENCE
ENGINEERING AND TECHNOLOGY

SUPPORTED LIPID BILAYERS WITH THIOLATED LIPIDS

M.Sc. THESIS

Abdulhalim KILIÇ

Department of Advanced Technologies

Molecular Biology & Genetics and Biotechnology Programme

Thesis Advisor: Assist. Prof. Dr. Fatma Neşe KÖK

JANUARY 2012

ISTANBUL TECHNICAL UNIVERSITY ★ GRADUATE SCHOOL OF SCIENCE
ENGINEERING AND TECHNOLOGY

SUPPORTED LIPID BILAYERS WITH THIOLATED LIPIDS

M.Sc. THESIS

Abdulhalim KILIÇ
(521081050)

Department of Advanced Technologies

Molecular Biology & Genetics and Biotechnology Programme

Thesis Advisor: Assist. Prof. Dr. Fatma Neşe KÖK

JANUARY 2012

İSTANBUL TEKNİK ÜNİVERSİTESİ ★ FEN BİLİMLERİ ENSTİTÜSÜ

**TIYOLLÜ LİPİTLERLE OLUŞTURULAN YÜZEY DESTEKLİ
LİPİT KATMANLAR**

YÜKSEK LİSANS TEZİ

**Abdulhalim KILIÇ
(521081050)**

İleri Teknolojiler Anabilim Dalı

Moleküler Biyoloji & Genetik ve Biyoteknoloji Programı

Tez Danışmanı: Yrd. Doç. Dr. Fatma Neşe KÖK

JANUARY 2012

Know thyself,

FOREWORD

First, I would like to thank my cheerful supervisor Assist. Prof. Dr. Fatma Neşe KÖK for her guidance. I am indebted her for giving me the chance in her research group.

I am grateful for guidance to Res. Assist. Ayşe Senem DONATAN, and Fatih İNCİ who have been helpful and friendly with me, for sharing their knowledge. I would also like to kindly thank to all members of our group and my labfriends.

On a personal note, I want to say “thank you” to my beloved family and my sweetheart fiancé for their love, belief in me and understanding.

This study was supported by ITU-BAP Project (34069).

December 2011

Abdulhalim KILIÇ
Molecular Biology and Genetics

TABLE OF CONTENTS

	<u>Page</u>
FOREWORD	ix
TABLE OF CONTENTS	xii
ABBREVIATIONS	xiii
LIST OF TABLES	xv
LIST OF FIGURES	xviii
SUMMARY	xix
ÖZET	xxii
1. INTRODUCTION	1
1.1 Purpose of Thesis	2
2. BACKGROUND INFORMATION	3
2.1 Lipids & Phospholipids	3
2.2 Self-Organization of Phospholipids Membranes	3
2.3 Lipid Vesicles	4
2.3.1 Preparation of liposomes	4
2.3.2 Classification of liposomes	8
2.3.3 Use of liposomes	10
2.4 Artificial Lipid Membranes	11
2.4.1 Supported lipid bilayers (SLBs)	12
2.5 Quartz Crystal Microbalance with Dissipation Monitoring (QCM-D)	13
2.5.1 The working principle	14
2.5.2 The dissipation	15
2.5.3 The overtones (harmonics)	17
2.6 Surface Plasmon Resonance (SPR)	18
2.6.1 The basic principle	18
3. MATERIALS & METHODS	21
3.1 Materials & Equipments	21
3.2 Methods	21
3.2.1 Preparation of unilamellar liposomes with extrusion method	21
3.2.2 Imaging of liposomes with optical microscopy	22
3.2.3 Measurement of adsorption kinetics	23
3.2.3.1 Preparation of gold surfaces	23
3.2.3.2 Quartz crystal microbalance	23
3.2.3.3 Surface plasmon resonance spectroscopy	25
4. RESULTS & DISCUSSION	27
4.1 Optical Microscopy of Liposomes	27
4.2 Interaction of PC Liposomes with Gold Surfaces	28
4.2.1 Unoxidized surfaces	28
4.2.2 Oxidized surfaces	30
4.2.2.1 Effect of the liposome concentration	31
4.2.2.2 Effect of the oxidation time	31

4.2.2.2 Comparison of the single pass system with the recycled one	31
4.3 Interaction of PC-DGPE Liposomes with Gold Surface	34
4.3.1 Adsorption of 0,1 % DGPE–PC liposomes.....	35
4.3.2 Adsorption of 1, 5, 50 % DGPE–PC and DGPE liposomes	37
4.4 The Effect of Na ⁺ and Ca ⁺⁺ Ions on the Multilayers	41
5. CONCLUSIONS & FUTURE WORKS	45
REFERENCES	47
APPENDICES	49
APPENDIX A	50
APPENDIX B.....	51
CURRICULUM VITAE	55

ABBREVIATIONS

ΔD	: Dissipation change
ΔF	: Frequency change
AFM	: Atomic Force Microscopy
BLMs	: Black Lipid Membranes
DSPE-PEG	: 1,2-distearoil-sn-glicerol-3-phosphoethanolamine-N-[amino(polyethylene glycol)-2000]
DGPE	: 1,2-Dipalmitoyl-sn-Glycerol-3-Phosphothioethanol
LUV	: Large Unilamellar Vesicles
LMV	: Large Multilamellar Vesicles
MVV	: Multivesicular Vesicles
MLV	: Multilamellar Vesicles
OLV	: Onion-like Vesicles
PBS	: Phosphate buffered saline
PC	: Phosphatidylcholine
PEG	: Polyethylene Glycol
RIU	: Refractive index unit
QCM	: Quartz Crystal Microbalance
QCM-D	: Quartz Crystal Microbalance with Dissipation Monitoring
SPR	: Surface Plasmon Resonance
SLBs	: Solid Supported Lipid Bilayers
SUV	: Small Unilamellar Vesicles
T_c	: Transition temperature

LIST OF TABLES

	<u>Page</u>
Table 2.1 : Some lipids used in liposome preparation	5
Table 2.2 : Liposome preparation methods.....	6
Table 3.1 : Different Lipid Solutions..	21
Table 4.1 : Summary of the experimental values with PC liposomes... ..	34
Table 4.2 : Summary of the experimental values with DGPE-PC and DGPE liposomes and BSA % 2.....	40

LIST OF FIGURES

	<u>Page</u>
Figure 2.1 : Chemical structure of L- α -Phosphatidylcholine.....	3
Figure 2.2 : The formation of liposomes membranes.	4
Figure 2.3 : Liposomes.....	4
Figure 2.4 : Mechanism and processing steps to generate various types of vesicles.	7
Figure 2.5 : Downsizing of vesicles by extrusion method.....	8
Figure 2.6 : Liposomes with different size and number of lamellae.....	9
Figure 2.7 : Types of liposomes according to their applications.	9
Figure 2.8 : Incorporation of nanoparticles within a liposome.	10
Figure 2.9 : Interaction ways between the cells and liposomes.	11
Figure 2.10 : Models of biological membranes.	12
Figure 2.11 : Formation of Supported Lipid Bilayers.....	13
Figure 2.12 : Vibrational motion of the crystal at its resonant frequency.	14
Figure 2.13 : The AT-cut quartz crystal electrodes and quartz crystals with different coatings.	15
Figure 2.14 : The changes at the frequency and the dissipation of the oscillating sensor crystal.....	16
Figure 2.15 : Example of raw data from a QCM-D experiment.	17
Figure 2.16 : Main Application areas of SPR Technology.	19
Figure 2.17 : Basics of SPR Phenomena.	19
Figure 3.1 : Chemical structure of DGPE.	21
Figure 3.2 : Liposomes were generated by an extruder.	22
Figure 3.3 : The fully assembled QCM and the electronic unit.....	23
Figure 3.4 : The reassembly of the measurement cell.....	24
Figure 3.5 : Surface Plasmon Resonance Spectrometer.	25
Figure 4.1 : Multilammellar vesicles observed under 10x objectives.....	27
Figure 4.2 : SUVs observed under 10x, 20x, 40x and 100x objectives.....	28
Figure 4.3 : Change in refractive index unit (RIU) versus time for the interaction of PC liposomes onto an unoxidized gold..	29
Figure 4.4 : Change in QCM resonant (normalized) frequency and dissipation versus time for the interaction of PC liposomes onto an unoxidized gold.	29
Figure 4.5 : Change in refractive index unit (RIU) versus time for the interaction of PC liposomes onto an oxidized gold.....	30
Figure 4.6 : Change in QCM resonant (normalized) frequency and dissipation versus time for the interaction of PC liposomes onto an oxidized gold.	31
Figure 4.7 : Δf_n and ΔD versus time for the interaction of PC liposomes (2x concentration of lipids) onto an oxidized gold	32
Figure 4.8 : Change in QCM resonant (normalized) frequency and dissipation versus time for the interaction of PC liposomes onto an 30' oxidized gold.	32
Figure 4.9 : Change in QCM resonant (normalized) frequency and dissipation versus time for the interaction of PC liposomes onto oxidized gold.	33

Figure 4.10 :	Vesicles remain intact and stable on the oxidized gold support.....	34
Figure 4.11 :	Change in refractive index unit (RIU) versus time for the interaction of 0,1 % DGPE-PC liposomes onto gold..	35
Figure 4.12 :	Δf_n and ΔD versus time for the adsorption of 0,1 % DGPE-PC liposomes onto gold	36
Figure 4.13 :	Change in QCM resonant (normalized) frequency and dissipation versus time for the interaction of 2 % BSA with gold.....	36
Figure 4.14 :	Rupture of the thiolated liposomes and formation of a lipid bilayer....	37
Figure 4.15 :	Change in refractive index unit (RIU) versus time for the interaction of 5, 10, 50 % DGPE-PC and DGPE liposomes onto gold...	37
Figure 4.16 :	Change in QCM resonant (normalized) frequency and dissipation versus time for the adsorption of 1 % DGPE liposomes onto gold..	38
Figure 4.17 :	Change in QCM resonant (normalized) frequency and dissipation versus time for the adsorption of 5 % DGPE liposomes onto gold..	38
Figure 4.18 :	Change in QCM resonant (normalized) frequency and dissipation versus time for the adsorption of 50 % DGPE liposomes onto gold..	39
Figure 4.19 :	Change in QCM resonant (normalized) frequency and dissipation versus time for the adsorption of DGPE liposomes onto gold.....	39
Figure 4.20 :	The formation of multilayers and the entrapped water between the layers.....	40
Figure 4.21 :	Change in refractive index unit (RIU) versus time for the effect of 0.01M Ca^{++} Ions on the Multilayers.....	41
Figure 4.22 :	Change in QCM resonant (normalized) frequency and dissipation versus time for the the effect of 0.01M Ca^{++} Ions on the Multilayers..	42
Figure 4.23 :	Change in QCM resonant frequency versus time for the the effect of 1 M Ca^{++} Ions on the Multilayers.....	43
Figure 4.24 :	Change in QCM dissipation versus time for the the effect of 1 M Ca^{++} Ions on the Multilayers	43
Figure 4.25 :	Change in QCM frequency and dissipation versus time for the effect of 0.1 M Na^+ ions on the multilayers.....	44

SUPPORTED LIPID BILAYERS WITH THIOLATED LIPIDS

SUMMARY

Biomimetic lipid bilayer platforms on solid supports are important model membrane systems to study the fundamental properties of biological membranes and their constituent lipid and protein molecules. They also offer a possibility for numerous practical applications, such as the construction of drug screening platforms based on membrane proteins. They allow the usage of surface-sensitive probes such as surface plasmon resonance (SPR) and acoustic sensors such as the quartz crystal microbalance with dissipation monitoring (QCM-D). Both QCM-D and SPR can supply information about adsorption events on surfaces and the properties of the resulting lipid films in real-time using frequency-dissipation changes (Δf - ΔD) and refractive index shift, respectively.

In this study, the aim was to determine the effect of thiolated lipids on the construction of these lipid bilayers on gold surfaces. For this, first a series of unilamellar liposomes (ca. 100 nm) with different phosphatidylcholine and 1,2-dipalmitoyl-sn-glycero-3-phosphothioethanol (PC-DGPE) lipid ratios were prepared by thin lipid film/extrusion method and their behaviour was explored in QCM-D. Interpretation of QCM-D data was also complemented with SPR analysis.

$\Delta D/\Delta f$ ratio obtained in QCM-D is a successful parameter to derive sensitive information about liposomal behavior during the binding process. The relatively high $\Delta D/\Delta f$ value of PC liposomes recycled in the system, which did not contain any thiol group, indicated the formation of a layer with high viscoelasticity and so the adsorption of intact vesicles onto the oxidized gold surface. These vesicles were washed rapidly from unoxidized surfaces whereas DGPE containing vesicles could interact with unoxidized ones thanks to their thiol (-SH) groups.

The low $\Delta D/\Delta f$ ratio for liposomes containing thiol-terminated lipids (0,1 % DGPE) suggested the rupture of the liposomes and formation of a lipid bilayer when compared with a $\Delta D/\Delta f$ value of the adsorbed Bovine Serum Albumin (BSA) monolayer on the surface, which could be used as a reference for a rigid layer. The overlapped frequency overtones observed also supported this observation. When the DGPE, thus the thiol, amount was increased, the overtone separation occurred.

The increase in the Δf values showed increased mass on the surface. DGPE lipid concentrations higher than 1 % have similar $\Delta D/\Delta f$ values indicating the build-up of rigid and compact phospholipid multilayers with low entrapped water content.

QCM-D and SPR were also used to evaluate the effects of cation (Na^+ , Ca^{2+}) presence in DGPE-PC multilayer composed of zwitterionic lipids. It was seen that

Ca^{++} solubilized and/or disrupted the multilayers and Na^{+} ions exhibit a much weaker but similar effect.

In conclusion, the addition of DGPE to PC liposomes was found to lead to the formation of a bilayer on the gold surface as opposed to the PC liposomes and the presence of thiol groups help the attachment of liposomes even to the unoxidized gold surface.

TİYOLLÜ LİPİTLERLE YÜZEYE BAĞLI LİPİT KATMANLAR

ÖZET

Yüzey destekli biyomimetik lipid katmanlar biyolojik membranların ve onları oluşturan lipid ve protein moleküllerinin temel özelliklerini araştırmak için önem arz eden model membran sistemleridir. Yüksek stabiliteye sahip olmaları üzerlerinde uzun dönemli deneylerin yapılmasına olanak sağlamaktadır. Örneğin, membran proteinlerini temel alan ilaç görüntüleme platformları oluşturma gibi çok sayıda pratik uygulamanın olabilirliğini de bizlere sunmaktadır. Bu model membran sistemleri, yüzey plazmon rezonans (SPR) gibi yüzeye hassas problemler ve disipasyon ölçümlü quartz kristal mikrotarazi (QCM-D) gibi akustik sensörlerin kullanımına da izin vermektedir.

QCM-D tekniğinin çalışma ilkesi bünyesindeki kuartz kristalin piezoelektrik özelliğine dayanmaktadır. Kuartz kristale uygulanan alternatif voltaj, kristalde mekanik bir salınımın tetiklenmesine neden olarak kristalin titreşim frekansını (f_0) oluşturur. Sonrasında yüzey üzerinde meydana gelecek kütleli değişimler (Δm) titreşim sıklığında değişimlere (Δf) neden olarak sensör yüzeyi üzerine tutunan moleküllerin tespit edilebilmesini olanaklı kılar. Bundan başka, yüzeye tutunan malzemeye su (veya diğer bir sıvı) molekülleri gerek direk hidrasyon gerekse filmin içinde tutulma şeklinde ek bir dinamik kütle olarak eşlik ediyorsa salınım yapan kristal bu katmanı viskoelastik bir hidrojel olarak algılayacaktır. Esnek bir filmin yüzeye tutunması ise, film katmanının kristalin salınımına tam olarak eşlik edememesine ve sensör salınımında azalmaya neden olacaktır. Salınımdaki azalma nedeniyle sistemden kaybolan enerjiyi (ΔD) ölçerek yüzeye tutunan malzemenin katı (rijit) veya esnek olup olmadığı, farklı katmanların yapısal farklılıkları veya adsorpsiyon sürecinde aynı katman içerisinde meydana gelen yapısal değişiklikler gerçek zamanlı olarak belirlenebilmektedir. Bu özellikleri ile QCM-D biyolojik sistemleri çalışmak için kullanılmaktadır.

Yüzey Plazmon Rezonans (SPR) yöntemi ise yüzeye eklenen moleküllerin yüzey kırınma indisini değiştirmesi ve bunun plazmon açısını (yansıyan ışığın en düşük olduğu açı) kaydırması esasına dayanmaktadır. Bu yöntemle yüzeye bağlanan veya yüzeyden uzaklaşan moleküller takip edilebilmektedir.

Bu çalışmada, tiyollü lipidlerin altın yüzeyler üzerinde lipid katmanlar oluşturmaındaki etkilerinin incelenmesi amaçlanmıştır. Bu amaçla önce phosphatidylcholine (PC) ve 1,2-dipalmitoyl-sn-glycero-3-phosphothioethanol (PC-DGPE) lipid çeşitlerini farklı oranlarda içeren lipozom (100 nm boyutlarında) dizileri ince lipid film/ekstrüzyon yöntemi ile üretildikten sonra yüzeye tutunum kinetikleri QCM-D ile incelendi. Elde edilen verilerin daha iyi yorumlanabilmesi için ayrıca SPR analizleri ile bütünleştirildi. Buna ek olarak ışık mikroskobu altında lipozom oluşumları görüntülendi.

Lipozomların davranışları temelde sensör yüzeyindeki elektriksel yüke ve lipid kompozisyonuna göre değiştiğinden ilk olarak, lipozomların oksitlenmiş ve oksitlenmemiş altın yüzeyler ile etkileşimleri lipozom konsantrasyonu, oksitlenme süresi, inkübasyon gibi parametreler değiştirilerek incelendi. Daha sonra ise farklı tiyol grubu oranındaki lipozomların oksitlenmemiş altın yüzeyler ile interaksyonu araştırıldı.

QCM-D ile elde edilen $\Delta D/\Delta f$ oranı yüzey etkileşimi süresince lipozomların davranışları hakkında hassas bilgiler çıkartabilmek için kullanılmakta olan önemli bir parametredir. Yüzeyde oluşan katmanı esneklik ve sertlik değerleri açısından değerlendirmemizi sağlayarak, oluşturulan lipid katman hakkında, tek tek ΔD ve Δf değerlerinin incelenmesinden daha fazla bilgi vermektedir.

Deney sonuçları, inkübe edilen PC lipozomlarının, ki hiç bir tiyol grubu içermemektedir, nisbeten büyük $\Delta D/\Delta f$ değerleri, yüksek esnekliğe sahip bir katmanın oluştuğunu, yani lipozomların oksitlenmiş altın yüzeyine deforme olmadan, bütün olarak tutunduklarına işaret etmektedir. Kutuplanan altın yüzeyi elektrostatik etkileşimin artmasını sağlayarak PC lipozomların yüzeye kolayca tutunabilmelerine neden oldu. Ayrıca artırılan lipozom konsantrasyonu ve altın yüzeyin maruz kaldığı oksidasyon süresi de yüzeye tutunan lipozom miktarını artırarak gerek lipozomlar içindeki gerekse de lipozomlar arası toplam sıvı miktarını artırarak $\Delta D/\Delta f$ değerinin de yükselmesine neden oldu.

Aynı tip lipozomların ise oksitlenmemiş altın yüzeye tutunamayıp hızlı bir şekilde yüzeyden yıkandıkları görüldü. Diğer yandan, DGPE içeren lipozomlar sahip oldukları tiyol (-SH) grupları nedeniyle oksitlenmemiş yüzeyler ile etkileşime girmektedirler.

% 0,1 oranında DGPE lipid tipi barındıran lipozomların sahip oldukları düşük $\Delta D/\Delta f$ oranları, bu lipozomların deforme olup parçalandıklarını ve çift katmanlı lipid yapı oluşturduklarını akla getirmektedir. Çünkü yüzeye rijit, tek katman şeklinde tutunmuş Bovine Serum Albumin (BSA) protein molekülleri de yaklaşık bir $\Delta D/\Delta f$ değerini göstermektedir. Ayrıca, tutunmakta olan bir filmin esnek olmayan yapısına işaret eden üst üste çakışmış frekans üst-tonları da bu gözlemi desteklemektedir. Lipozomlardaki DGPE, yani tiyol grubu oranı arttırıldığında ise frekans üst-tonlarının da ayrıldığı gözlemlendi.

% 1'den daha fazla DGPE konsantrasyonlarından elde edilen birbirine yakın $\Delta D/\Delta f$ değerleri, rijid, sıkı ve düşük miktarlarda da su içeren çoklu lipid katmanlarının oluştuğunu göstermektedir. DGPE oranıyla paralel olarak artan Δf değeri de yüzeyde miktarı artan bu kütleye ayrıca işaret etmektedir.

Ayrıca QCM-D ve SPR kullanarak, katyonik bir iyon olan Na^+ ve Ca^{++} 'in zwitteriyonik lipidlerden oluşan DGPE-PC çoklu katmanları üzerindeki etkileri de değerlendirildi. Bulgular, çoklu lipid katmanlarında Ca^{++} iyonları nedeniyle çözünme ve bozunma meydana geldiğine işaret etmektedir. Na^+ iyonları da benzer fakat daha zayıf etkiler göstermiştir.

Kısacası, PC lipozomlarının yapısına DGPE lipidlerinin eklenmesi $\Delta D/\Delta f$ oranını önemli derecede azalttığı, yani PC-DGPE lipozomlarının parçalanıp yüzeye yayılarak çift katmanlı lipid yapısı oluşturdukları fikrini vermektedir.

1. INTRODUCTION

The current interest and need in reconstituting biomimetic lipid bilayer platforms to be used in the investigation of cell-cell and/or cell-substrate interactions aims linking the biological world with the field of surface science [1]. Practically, supported membranes allow the biofunctionalization of inorganic surfaces. Potential applications include biosensors, the acceleration and improvement of medical implant acceptance, programmed drug delivery, and the production of catalytic interfaces [2].

Successful construction of these systems would not only improve our understanding of basic cellular functions but also allow us to develop biotechnological tools, biomedical devices, or biofunctional materials. To do this, it is paramount to develop reliable methods to control the formation of solid supported lipid membranes and to find effective ways to incorporate, and address biological entities, from molecules to cells [1].

There are various surface sensitive techniques to characterize these systems. The simplest way to examine their quality and integrity is to look for their uniform appearance on a standard epifluorescence microscope. Many artifacts can be detected readily and eliminated with this very simple test. Higher-resolution images can be obtained by atomic force microscopy (AFM) or near-field fluorescence microscopy (NSOM). These techniques are useful to detect small defects in the 10 to 500 nm range that might escape detection by standard wide-field optical microscopy. Binding of proteins to supported bilayers may be studied quantitatively by total internal reflection fluorescence microscopy (TIRFM). Fluorescence recovery after photobleaching (FRAP) and single particle tracking (SPT) are two common techniques to determine the diffusion of fluorescently labeled lipids or proteins in supported bilayers. Secondary structure and orientation of membrane proteins in supported bilayers are conveniently measured by polarized Fourier-transform infrared (FTIR) spectroscopy [3].

Both surface plasmon resonance (SPR) and ellipsometry, being optical techniques can provide information about adsorption events on surfaces and the properties of the resulting films. In particular, both techniques can quantify adsorbed masses in real-time. Quartz crystal microbalance with dissipation monitoring (QCM-D) tool is especially attractive in artificial lipid bilayer studies providing a simple way of characterizing the adsorption kinetics of intact liposomes or fused bilayer/multilayer formation since the frequency change in the sensor (Δf) reflects film mass and dissipation (ΔD) correlates to viscoelastic properties [4-6].

1.1 Purpose of Thesis

In this study, the aim was to determine the effect of thiolated lipid presence on the construction of supported lipid bilayers on gold surfaces. For this, unilamellar liposomes with different thiolated phospholipid content (phosphatidylcholine (PC) and 1,2-Dipalmitoyl-sn-Glycero-3-Phosphothioethanol (DGPE); 0,1-100 % DGPE) was used. Quartz Crystal Microbalance with Dissipation Monitoring (QCM-D) that is commonly used for real-time, label-free evaluation of binding and interactions of biological molecules in liquid environment was used to investigate the liposomal binding and assessment of mass and viscoelastic properties of thin lipid films. Interpretation of QCM-D data was also complemented with surface plasmon resonance (SPR) analysis.

2. BACKGROUND INFORMATION

2.1 Lipids & Phospholipids

Lipids are small hydrophobic or amphiphilic molecules used in the living systems for many biological functions including energy storage, structural components of cell membranes, and signaling pathways.

Major constituents of cell membranes are phospholipids containing a diglyceride, a phosphate group, and a simple organic molecule such as choline. Phospholipids have at least one negative charge at a neutral pH [7]. The most common natural phospholipid is the phosphatidylcholine (PC) that is an amphipathic molecule originated mostly from animal (hen egg) (Figure 2.1). Its primary role is to provide a structural framework for the membrane and maintain the permeability barrier. It also plays a role in membrane mediated cell signaling. In addition, there are different types of phospholipids, such as phosphatidylethanolamine (cephalin) that has an ethanolamine residue instead of choline, phosphatidylserine has a serine residue, and etc. [7, 8].

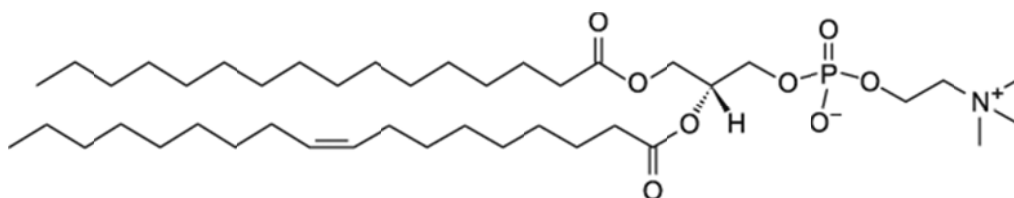


Figure 2.1 : Chemical structure of L- α -Phosphatidylcholine

2.2 Self-Organization of Phospholipids Membranes

Because of the amphiphilic nature of phospholipid molecules (a hydrophilic head, the phosphate head group, connected to a hydrophobic tail, an aliphatic chain), a rapid and spontaneous association of the molecules occur when they are transferred into an aqueous solution. The aliphatic parts of each layer are positioned towards each other and the hydrophilic heads are faced either to the bulk water or to the

inside part of the closed structure. That self-organization of the phospholipids results in the formation of the bilayer structure (Figure 2.2) [9].

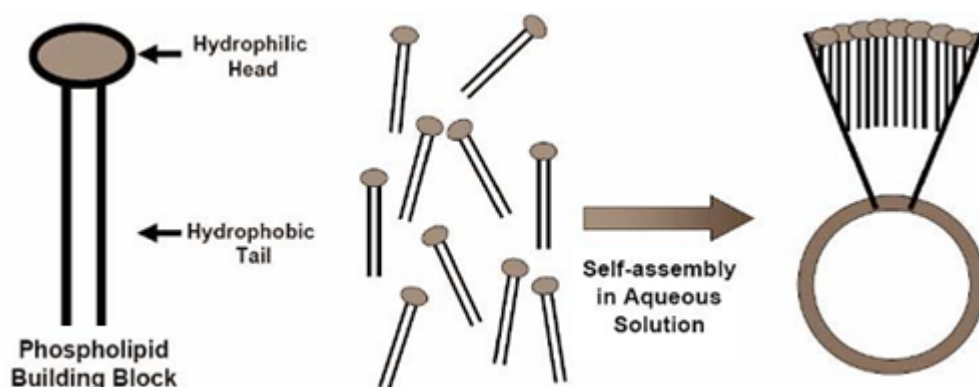


Figure 2.2: The formation of liposome membranes by the self-assembly of phospholipids in aqueous solution.

2.3 Lipid Vesicles

In an aqueous system, depending on the concentration of the lipid, clusters of lipids form micelle, liposome, or lipid bilayer structures. Phospholipids with long or two alkyl chains do not form micelles but organize into bilayer structures. Liposomes are artificial lipid vesicles defined as lipid bilayers surrounding one or more internal aqueous compartments (Figure 2.3) [10].

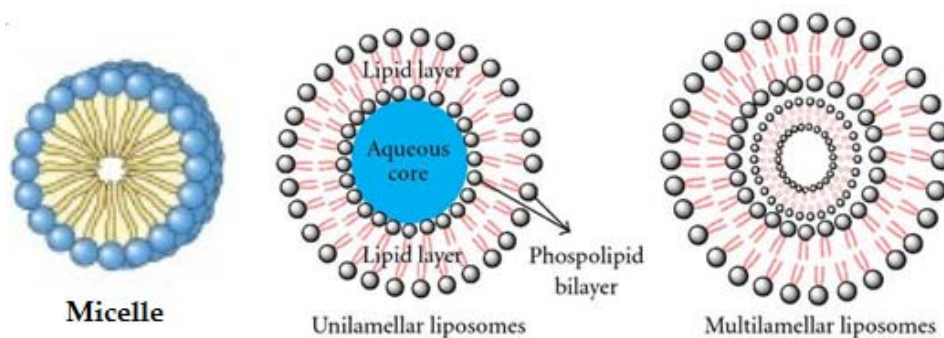


Figure 2.3: Liposomes.

2.3.1 Preparation of liposomes

Liposomes can be prepared with a variety of phospholipids (natural, modified, semi-synthetic, fully-synthetic) (Table 2.1). The most widely used lipids are phosphatidylcholine, phosphatidylethanolamine and phosphatidylserine which have been used either individually or in combination with cholesterol. Cholesterol allows the close packing of phospholipids in bilayers even above the transition temperature

(Tc). It also reduces the permeability by filling up holes or disruptions of the bilayers to encapsulated compounds. Negatively charged lipids, such as stearylamine, are usually used in order to introduce a surface charge to the liposomes [11, 12].

Table 2.1 : Some lipids used in liposome preparation

Neutral	Phosphatidylcholine (PC)
	Phosphatidylethanolamine (cephalin) (PE)
	1,2-dimyristoyl-sn-glycero-3-phosphocholine (DMPC)
	Dipalmitoyl phosphatidylcholine (DPPC)
Negatively charged	Phosphatidylserine (PS)
	Phosphatidylinositol (PI)
	Phosphatidylglycerol (PG)
	Phosphatidic acid (phosphatidate) (PA)
Positively charged	1,2-dioleoyl-3-trimethylammonium-propane (DOTAP)
	1,2-di-O-octadecenyl-3-trimethylammonium propane (DOTMA)

There are many different strategies for the preparation of liposomes, which can be classified into three main groups (Table 2.2). Additional methods developed, such as freeze thawing, freeze drying, and extrusion, are all based on preformed vesicles [13].

The lipid film method is still the simplest procedure for the liposome formation but is limited because of its low encapsulation efficiency. In this method, phospholipid solution dissolved in hydrophobic organic solvent is dried to form a thin film layer and it is re-solvated in an aqueous solution, and “onion-like” (OLV), larger micron-scaled multilammellar vesicles (LMV) are formed. These “multi-walled” structures can be easily converted to small unilammellar vesicles (SUV) of single bilayers with sizes that range from few hundreds of nm to 50 nm, upon sonication or extrusion (Figure 2.4) [9, 14].

Table 2.2 : Liposome preparation methods.

Method	Vesicles
<i>Mechanical methods</i>	
Vortex or hand shaking of phospholipid dispersions	MLV
Extrusion through polycarbonate filters at low or medium pressure	OLV, LUV
Extrusion through a French press cell “Microfluidizer” technique	Mainly SUV
High-pressure homogenization	Mainly SUV
Ultrasonic irradiation	SUV
<i>Methods based on replacement of organic solvent(s) by aqueous media</i>	
Removal of organic solvent(s)	MLV, OLV, SUV
Use of water-immiscible solvents: ether and petroleum	MLV, OLV, SUV
Ethanol injection method	LUV
Ether infusion (solvent vaporization)	LUV, OLV, MLV
Reverse-phase evaporation	
<i>Methods based on detergent removal</i>	
Gel exclusion chromatography	SUV
“Slow” dialysis	LUV, OLV, MLV
Fast dilution	LUV, OLV
Other related techniques	MLV, OLV, LUV, SUV

In ultrasonication method, aqueous dispersion of phospholipids are disrupted with an either bath or a probe sonicator and this procedure will usually yield SUVs with diameters down to 15-25 nm. Similar to the ultrasonication methods, homogenization techniques have been used to reduce the size and number of lamellae of multilamellar liposomes [13].

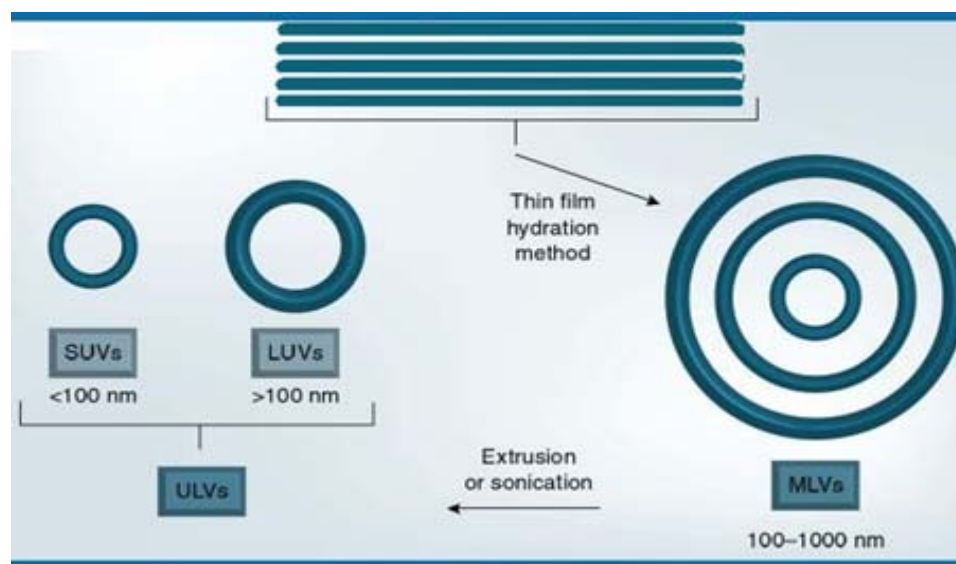


Figure 2.4 : Mechanism and processing steps to generate various types of vesicles.

In extrusion technique, that is the most prominent scalable downsizing method, lipid suspension is forced through a polycarbonate filter with a defined pore size to yield uniformed particles. As it is in all procedures for downsizing LMV dispersions, the extrusion should be done at a temperature above the transition temperature (T_c) of the lipid. Below T_c , the lipids have a tendency to form crystalline structures that cannot pass through the pores. Extrusion through filters with 100nm pores typically yields large, unilamellar vesicles (LUV) with a mean diameter of 120-140nm. Mean particle size also depends on lipid composition (Figure 2.5) [15].

A common practice is to subject MLVs to freeze-thaw cycles prior to extrusion, which increases the proportion of unilamellar vesicles in preparations. The freezing and thawing cycle has been shown to cause internal lamellae of MLVs to separate and vesiculate, which probably reduces the number of closely associated bilayers forced through pores together, thus reducing the formation of oligolamellar vesicles [16].

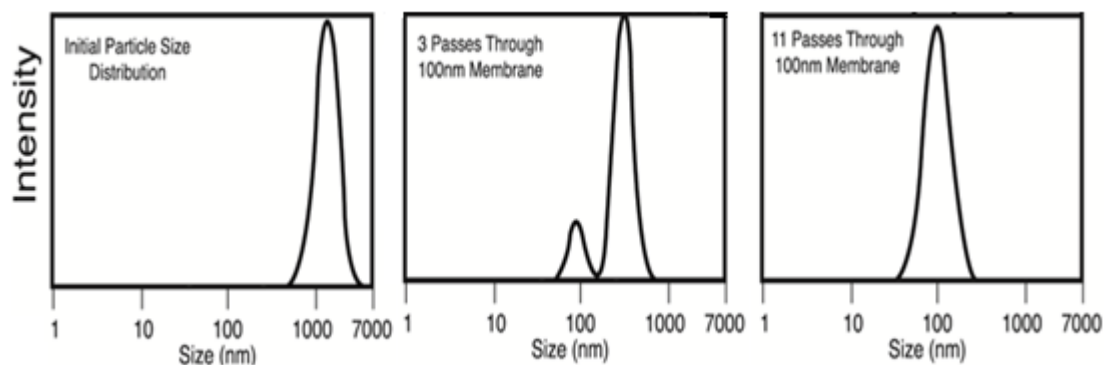


Figure 2.5 : Downsizing of vesicles by extrusion method.

2.3.2 Classification of liposomes

Liposomes can be classified based on various characteristics, according to size, lamellarity, lipid composition, surface charge and their functionality. Below, two of them are mentioned.

Based on their size and lamellarity

The size of liposomes varies between 25 nm and few micrometers and the thickness of a single lamella is around 4 nm. Multivesicular vesicles (MVV) carry several smaller liposomes inside one big vesicle. Multilamellar vesicles (MLV), in an onion-like arrangement consists several (up to 14) lipid layers separated from one another by a layer of aqueous solution. These vesicles are over several hundred nanometers in diameter. Small unilamellar vesicles (SUV) are surrounded by a single lipid layer and are 25–100 nm in diameter. Large unilamellar vesicles (LUV) are as for a very heterogenous group of vesicles that, like the SUVs, are surrounded by a single lipid layer. The diameter of these liposomes is very broad, from 100 nm up to cell size (giant vesicles) (Figure 2.6) [10, 17].

Based on their functionality

The liposomes can also be classified as conventional liposomes, long-circulating liposomes, immunoliposomes and cationic liposomes based on their functionality introduced for different applications (Figure 2.7). Conventional liposomes are composed of neutral and/or negatively charged phospholipids and/or cholesterol. They can vary in size, lipid composition, surface charge and lamellarity. Long-circulating or also called 'stealth' or 'sterically stabilized' liposomes are developed by coating their surface with a polymer, most popularly attaching hydrophilic polymer

polyethylene glycol (PEG) covalently to the outer surface. Immunoliposomes have specific antibodies on their surface to enhance the efficiency of drug delivery to the target site. They can be coated with PEG, thus their chance to reach target sites would be improved. Cationic liposomes are used in DNA-RNA delivery [18, 19].

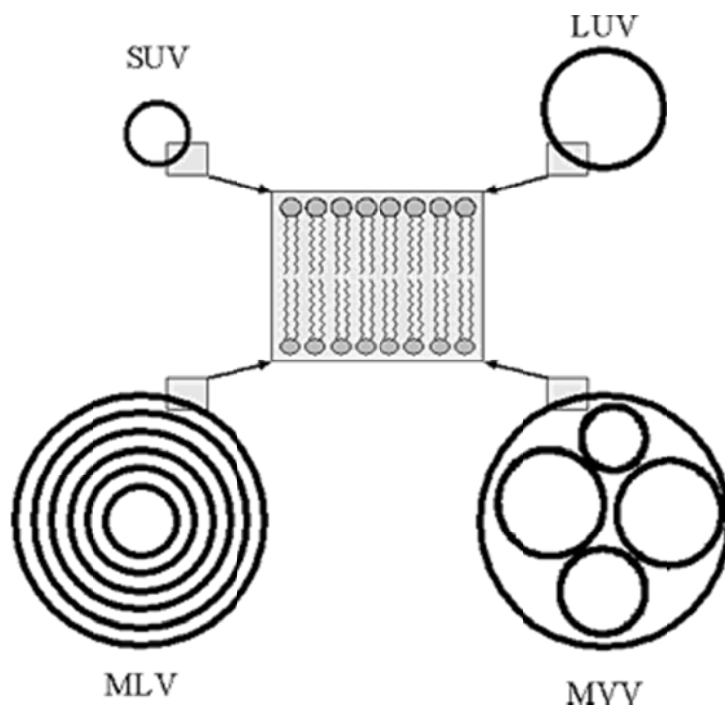


Figure 2.6 : Liposomes with different size and number of lamellae.

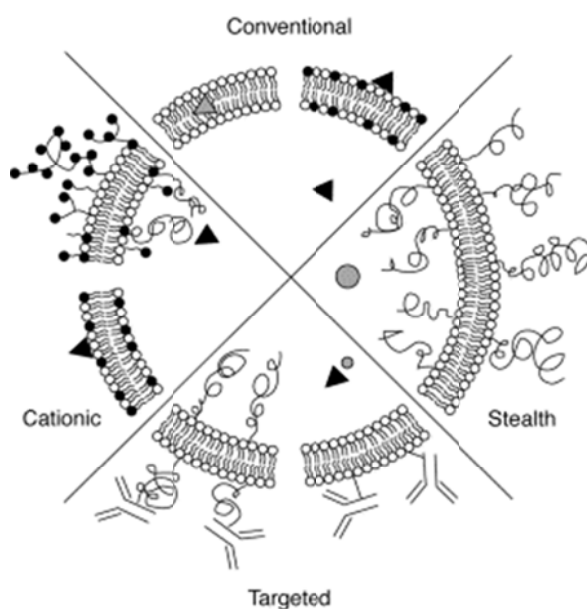


Figure 2.7 : Types of liposomes according to their applications.

2.3.3 Use of liposomes

Liposomal vesicles are prepared from various lipid types (see Table 2.1) identical to those present in most biological membranes. Basic studies on liposomal vesicles resulted in numerous methods of their preparation and characterization. The discovery of liposomes leads the scientists to use them as cell membrane models. Also, the ability of liposomes to encapsulate hydrophilic solutes in their internal aqueous spaces and/or incorporate the hydrophobic molecules within the lipid bilayer was led to the idea of loading and carrying antitumor-antifungal-antimicrobial drugs, genes, enzymes, proteins, vitamins, vaccines, as well as imaging agents into liposomes or polymers or targeting ligands (e.g. antibodies) on their surface (Figure 2.8) [17, 20, 21].

Liposomes are now most clinically established nanometer-scale delivery systems by the outstanding profile over the other systems due to their biocompatibility, biodegradability, reduced toxicity and capacity for size and surface manipulations [21]. They are attractive delivery mechanisms in a number of useful applications. They are especially useful for increasing the lifetime of drugs in the blood, targeting and delivering very potent and very toxic drugs to given specific locations [22].

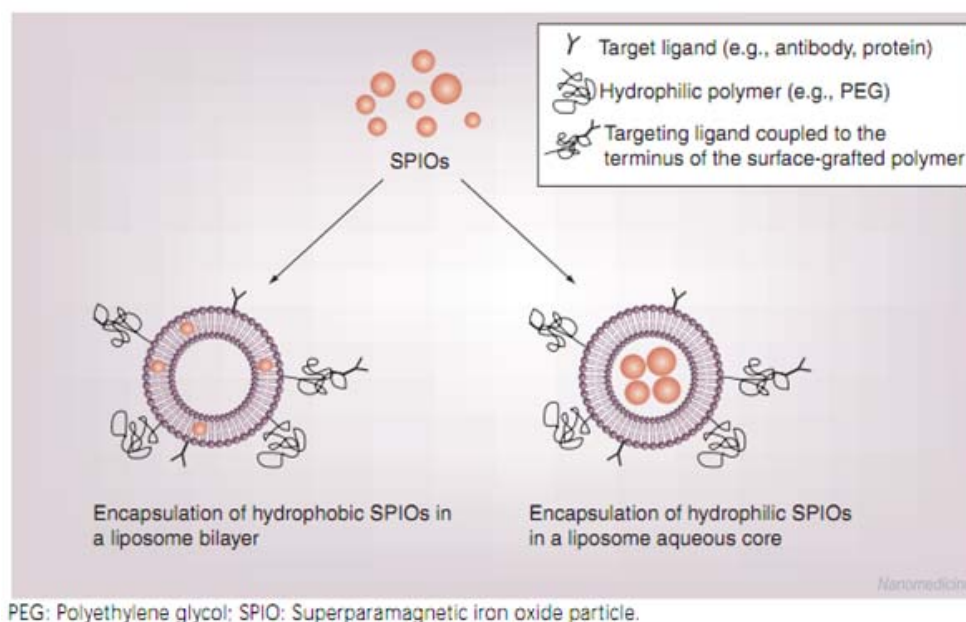


Figure 2.8: Incorporation of superparamagnetic iron oxide nanoparticles within a liposome bilayer (left) or a liposome aqueous core (right).

There are several different interaction ways between the cells and liposomes (Figure 2.9). They may merely bump into the surfaces of cells, bind weakly and then any drugs carried inside the liposome can slowly leak out, and by this, a small but consistent dose to the local area is provided. Moreover, the liposomes could be taken into cell by the normal endocytosis mechanisms. They pass through the lysosomes, internalized molecules are digested, the liposome is degraded and the molecules inside are released. Finally, in special cases, liposomes can be designed to fuse with the cell surface. They then unload their contents directly into the cell and incorporate their lipids directly into the cell membrane [22].

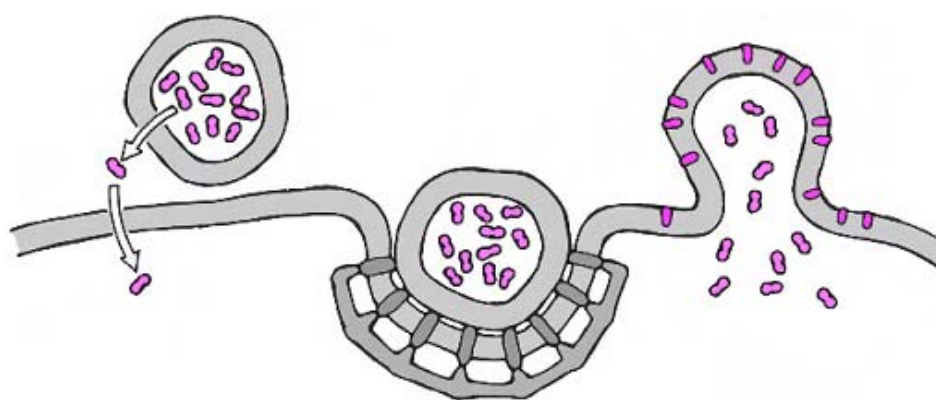


Figure 2.9 : Interaction ways between the cells and liposomes.

2.4 Artificial Lipid Membranes

Biological membranes are crucial in cell life as being selectively permeable barriers and having special sites of communication between the inside and outside of the cellular worlds. Because of the complexity of biomembranes, there is a clear need to develop model membrane systems, where one or a few membrane components can be isolated and studied. Therefore, artificial lipid membrane studies are crucial to comprehend the molecular events taking place at biological membranes and to explore possible biotechnological applications. These studies must sustain the structure, fluidity of the lipid bilayer and the physiological reality, as well as the structure and function of reconstituted membrane proteins [1, 3].

The current knowledge of the molecular processes occurring at biological membranes mainly based on the studies with the biological membrane models including liposomes, giant vesicles in solution, lipid monolayers, black lipid films,

lipid bilayers between two aqueous phases and solid supported membranes (Figure 2.10) [1].

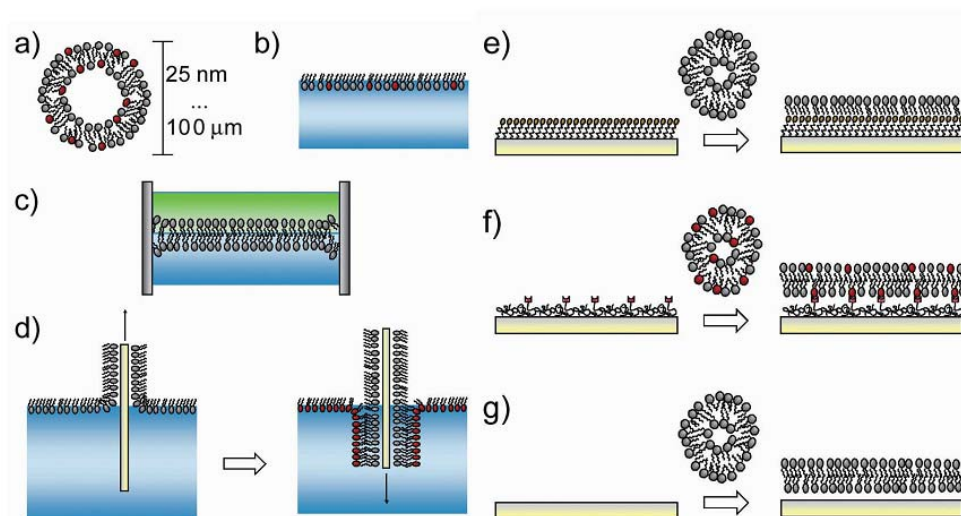


Figure 2.10: Models of biological membranes. (a) liposomes (25 nm to 100 μm in diameter); (b) lipid monolayers at the air-water interface; (c) black lipid membranes suspended over an aperture between two aqueous phases; (d) Langmuir-Blodgett method allowing the transfer of lipid mono- and multi-layers from the air-water interface to a solid support; (e) self-assembled monolayer on glass/gold/silica surface; (f) polymer cushioned bilayer; (g) spontaneous spreading of liposomes on surface.

2.4.1 Supported lipid bilayers (SLBs)

Solid supported lipid bilayers (SLBs) are widely studied membrane mimicking models that formed spontaneously when liposomes in solution encounter a solid surface. There are some different pathways that the liposomes could follow after facing the surface (Figure 2.11). Adsorption (1) and consequent deformation of liposome (likely flattening) is the first step. If deformation is large enough, some liposomes may rupture (2-5) to form a continuous lipid bilayer on the surface. Vesicles can rupture individually (2), or after interaction with other vesicles (3, 4) and/or with bilayer patches (5). The interactions are dependent on the surface charge, structure, smoothness of the solid support; the composition, charge and size of the liposome and finally the pH and ionic strength of the aqueous solution [1, 23].

Solid supported lipid bilayers have high stability and allow the use of surface sensitive characterization tools that are not possible to use in bulk solution. Unlike black lipid membranes (BLMs), they remain largely intact even when subjected to high flow rates or vibration and the presence of holes will not destroy the entire

bilayer. Because of this stability, long-term experiments are possible with SLBs, but not for BLMs [24].

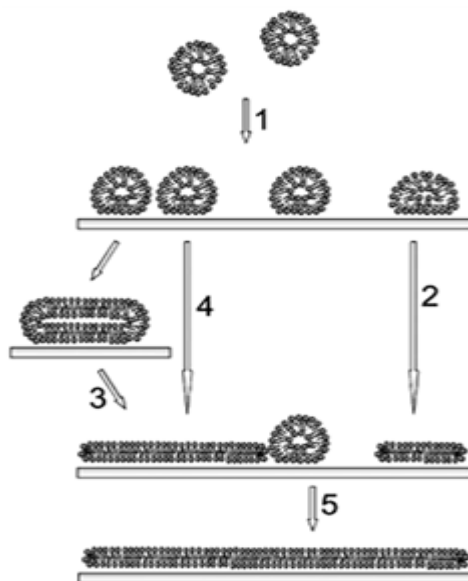


Figure 2.11 : Formation of SLB's by (1) adsorption and (2-5) rupture of liposomes, followed by bilayer formation.

Supported lipid bilayers are valuable in the study of the characteristics and behavior of membrane-bound proteins, membrane mediated cellular processes, protein-lipid interactions, and biological signal transduction [2, 25]. Applications of supported membranes on solid surfaces potentially include biosensors, programmed drug delivery devices, surface modification of medical implants, bioresorbable material scaffolds supporting cell attachment and growth (tissue engineering), and the production of catalytic interfaces. In addition, they allow the use of most of the surface-sensitive techniques [26-28].

The surface-sensitive methods such as atomic force microscopy (AFM), surface plasmon resonance (SPR) and quartz crystal microbalance (QCM), employing optical or mechanical sensing, are among popular methods for physical, chemical and structural characterization of lipid layers within aqueous environments [1].

2.5 Quartz Crystal Microbalance with Dissipation Monitoring (QCM-D)

QCM-D is a label-free method intensively used in recent years to study various biological systems such as cells, vesicles, proteins in liquid environment and their interactions with different natural or artificial interfaces. This technique is

qualitatively capable to detect the adsorption of biomolecules with their subsequent structuring when adsorbed on the sensor surface [29]. Various biologically relevant questions have been investigated by QCM-D, such as the activity of enzymes, the hybridization of nucleotide strands, functional aspects of supported lipid membranes, DNA-drug interactions, protein cross-linking or the adhesion and spreading of cells [30].

Studying vesicle interactions with solid surfaces using the QCM-D technique is initiated by Kasemo and coworkers [1998] and vesicle fusion became an established tool to form SLBs due to the ability of QCM-D to characterize the entire process in real-time, including the quality as well as the kinetic analysis of the formed bilayer [31].

2.5.1 The working principle

Pierre and Jacques Curie discovered in 1880 that when a mechanical stress is applied on the surface of quartz, an electrical potential could be generated and when the quartz is subjected to an electric field, it mechanically deforms. This effect is called as the piezoelectric effect [32]. The term piezoelectric is derived from the Greek piezein-elektro or ‘pressure-electric’ and piezoelectricity is the term to define the coupling of material’s mechanical and electrical behaviors. By applying a sufficient alternating voltage with a frequency close to the resonant frequency (f_0) of the quartz crystal, a mechanical oscillation can be excited (Figure 2.12) [33, 34]. When voltage is applied between the electrodes, a reorientation of the dipoles inside the quartz leading to shear deformation of the crystal is resulted and this eventually induces an acoustic wave traveling across the crystal and reflecting from the quartz surfaces [35].



Figure 2.12 : Applying an alternating electric field causes vibrational motion of the crystal at its resonant frequency.

Today, a circular piece of quartz is sandwiched between two metal electrodes is used mostly in QCMs. The “AT cut” quartz is generally used to give favorable properties

relating to stability (low temperature coefficients and a purely shear mode of oscillation (Figure 2.13) [34].

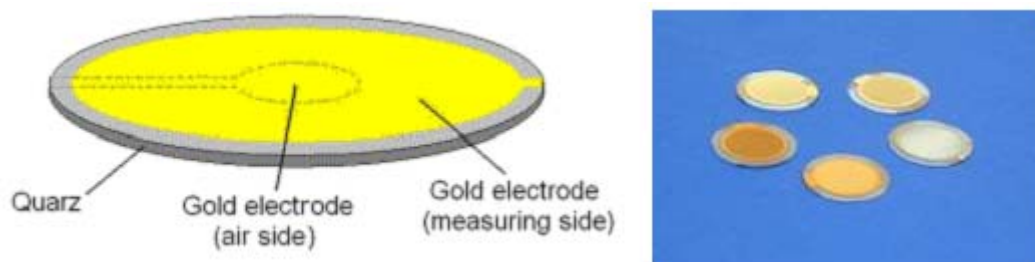


Figure 2.13 : The AT-cut quartz crystal electrodes and quartz crystals with different coatings.

According to the basic theory of QCM developed by Sauerbrey (1959), the frequency change (Δf) of a quartz crystal resonator was a linear function of the adsorbed mass (Δm) (equation 2.1) [36] if the film is evenly distributed over the active area of the crystal (uniform), thin compared to the thickness of the crystal, rigid and coupled to the crystal such as it can be treated as an extension of the quartz crystal. [37]

$$\Delta m = C \cdot \Delta f \text{ (Sauerbrey equation)} \quad (2.1)$$

C, mass sensitivity constant equals to $\sim -17.7 \text{ Hz ng/cm}^2$ for a 5-MHz crystal depending on the thickness and the density of quartz [35].

Successful application of QCM in liquid environments beginning from 1980 has led to a dramatical increase in various applications in biotechnology and in particular in biosensor field. However, the incorporation of viscosity and elastic contribution (dampening of the resonator) to the frequency change of the liquid phase was violated the assumption of the Sauerbrey relation and lead researchers to new ways to reinterpret the data and to characterize mass deposits with frictional dissipative losses because of their viscoelastic character (Figure 2.14) [6, 34].

2.5.2 The dissipation

The QCM-D senses all material that is mechanically deformed. Moreover, oscillating quartz crystals sense a layer as a viscoelastic “hydrogel” when water (or other liquid) couples to the adsorbed material as an additional dynamic mass via direct hydration and/or entrapment within the adsorbed film. If a film layer is viscoelastic or ‘soft’, it will not fully couple to the oscillation of the crystal, and will dampen the crystal’s

oscillation results in a decrease of the quality factor, Q , of the crystal. The Q -factor contains all the information about how well the quartz crystal is resonating in the surrounding media. This means that the influence of all kind of adsorbed layers on the quartz crystal or liquids in contact with the quartz crystal surface is reflected in the Q -factor [6, 38]. The damping or dissipation (D) which is the inverse of Q , includes information on the film's viscoelasticity. D is defined as the ratio of energy lost (dissipated) during one oscillation cycle to the total energy stored in the oscillator (equation 2.2) [33]:

$$D = E_{\text{lost}} / 2\pi E_{\text{stored}} \quad (2.2)$$

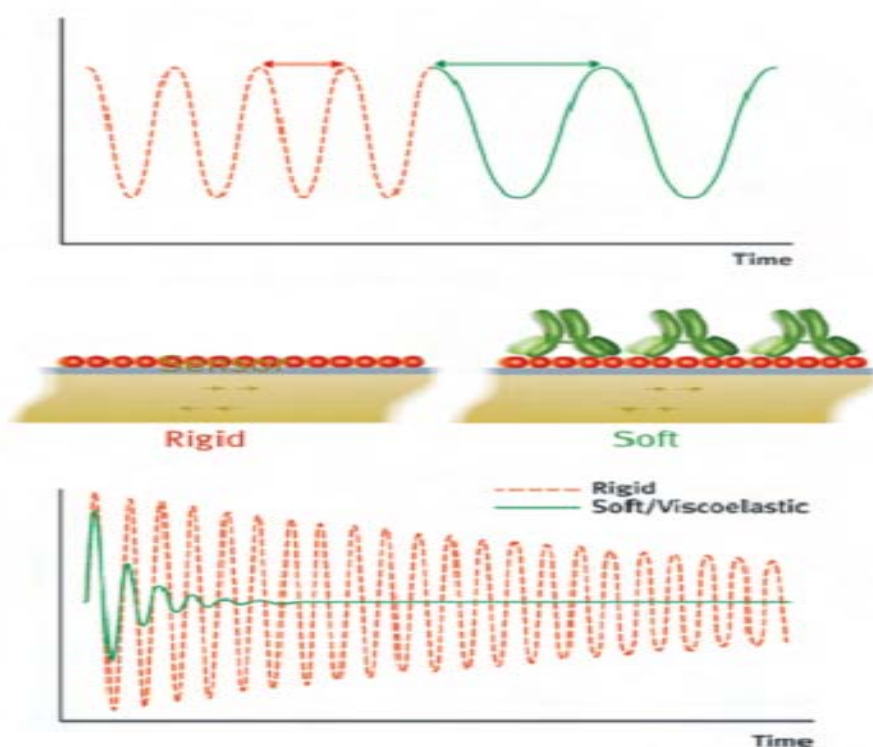


Figure 2.14 : The top diagram illustrates how the frequency of the oscillating sensor crystal (gold) changes when the mass is increased by addition of a molecular layer. Here soft molecules (green) are added to a layer of rigid molecules (red). The bottom diagram shows the difference in dissipation signal generated by a rigid (red) and soft (green) molecular layer on the sensor crystal.

Hence, the rigidity or viscoelasticity (softness) of the adsorbed film and structural differences between different adsorbed systems, or structural changes in the same film during the actual adsorption process can be determined by measuring the dissipation. Briefly, if a rigid structure, like lipid membrane, is formed on the

surface, low amount of water would couple to the molecules and the film would have a low dissipation value. On the other hand, if a viscoelastic layer formed on the surface (e.g. liposome adsorption), it would be highly dissipative. An example of a typical Δf and ΔD data versus time for both types of molecules can be seen in Figure 2.15 [34].

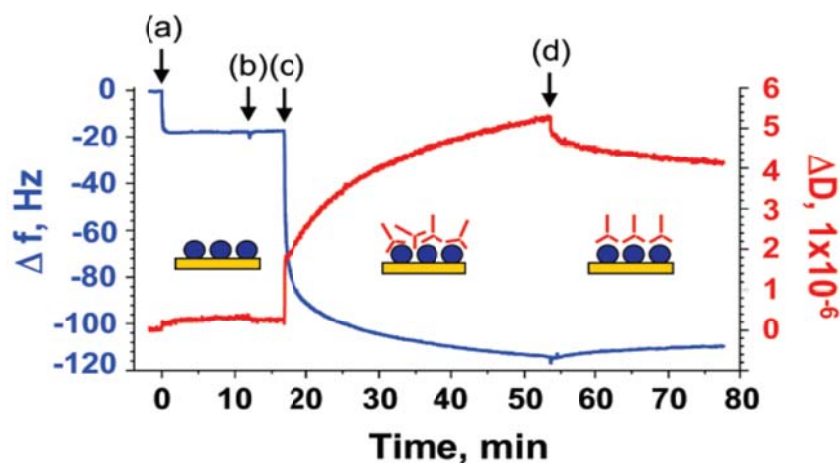


Figure 2.15 : Example of raw data from a QCM-D experiment. Injection of a rigid (a) and soft (c) molecules. Steps (b) and (d) correspond to buffer rinses. Frequency changes (Δf) are shown in blue on the left axis and dissipation changes (ΔD) are shown in red on the right axis.

2.5.3 The overtones (harmonics)

In some cases, the adsorbed film could be so soft that the upper region away from the crystal surface, do not couple to the oscillation of the crystal sensor. Measuring both dissipation and frequency at several harmonics ($n = 3, 5, \dots$) allows modeling the experimental data and determining parameters such as mass, thickness, density or visco-elasticity [39].

Different overtone frequencies probe the adlayer at different depths. The detection range decreases with increasing overtone number. Therefore, the different overtones supply data about the homogeneity of the adsorbed films and it is possible to solve the properties of different layer combinations. In addition, higher overtones provide an increased sensitivity and signal-to-noise ratio, which is good when better sensitivity is required [35].

2.6 Surface Plasmon Resonance (SPR)

Surface plasmon resonance (SPR) is one of the most widely used optical technique for various biological and chemical sensing applications. Using SPR, optical properties (refractive index, dielectric constants, extinction coefficient) and thickness, porosity and conductivity of thin layers, surface density/concentration of molecules; surface reactions (Binding/interaction kinetics, affinity, specificity, binding/interaction enthalpy and activation energy) and surface adsorption/desorption (biomolecules, polymers/polyelectrolytes, surfactants and lipids) can be characterized (Figure 2.16) [40, 41].

2.6.1 The basic principle

Freely mobile electrons on a metal surface generate a free electron gas. This free electron gas can be excited by light under specific conditions. The penetration of the electromagnetic field component of light to the metal layer causes the transfer of energy to the metal's free electrons, and results in as plasmons on the metal surface. Surface plasmons are electromagnetic waves confined to the surface and penetrate a short distance ($\sim \frac{1}{2}$ wavelengths) propagating parallel along a metal/dielectric interface, and they are extremely sensitive to refractive index n and its changes. The exact position of resonance provides information on the optical properties and also mass/coverage/thickness of the interfacial layers. The interactions at the gold surface alter the surrounding environment of thin metal film, leading shifts in the plasmon resonance condition and in the refractive index of the surface. Change in the refractive index is simultaneously detected by a sensor and plotted as response (resonance units – RU) versus time (Figure 2.17) [41-43].

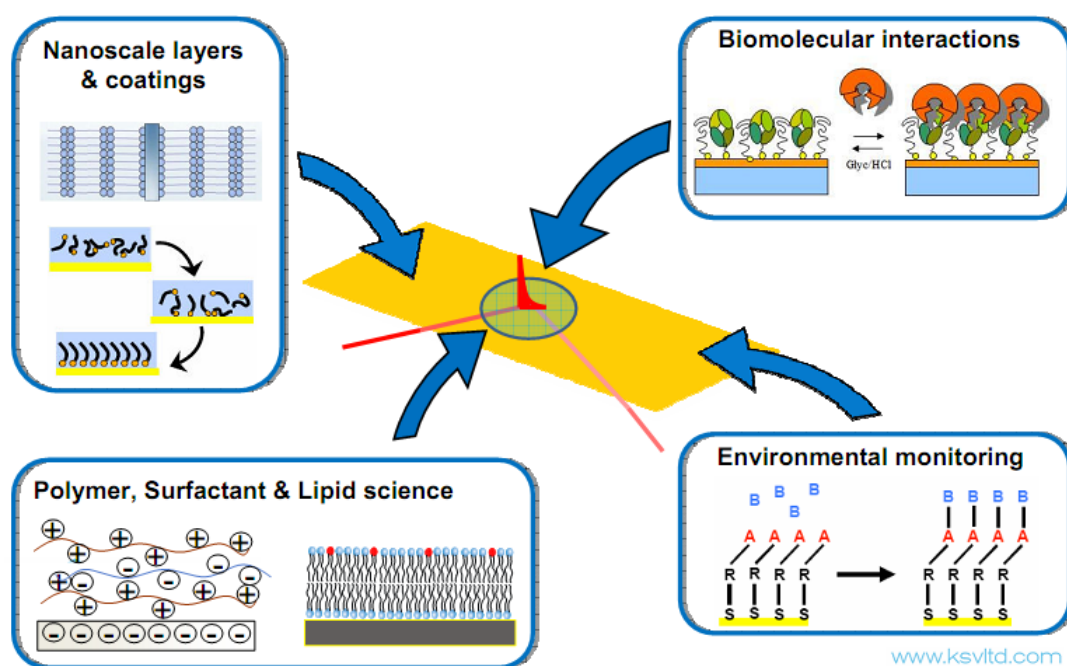


Figure 2.16 : Main Application areas of SPR Technology

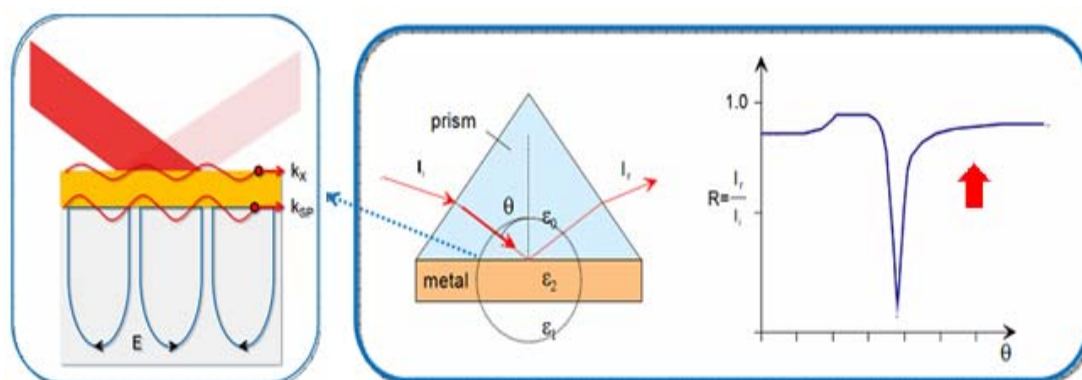


Figure 2.17 : Basics of SPR Phenomena

3. MATERIALS & METHODS

3.1 Materials & Equipments

The laboratory materials, equipments and chemicals used in the experiments were listed in Appendix A and B.

3.2 Methods

3.2.1 Preparation of unilamellar liposomes with extrusion method

Preparation of stock solutions

Phosphatidylcholine (PC) (Figure 2.1), and 1,2-Dipalmitoyl-sn-Glycero-3-Phosphothioethanol (DGPE) lipids (Figure 3.1) were dissolved separately in organic solvent (chloroform) at +4°C as a stock solution (1 mg/mL), aliquoted and stored at -20°C.

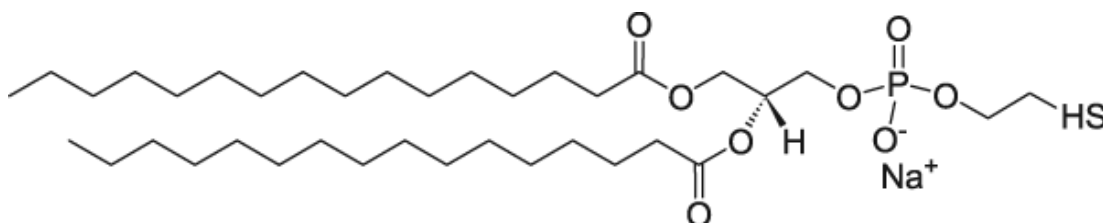


Figure 3.1 : Chemical structure of DGPE

Preparation of thin lipid film

To prepare thin lipid film layer, lipid solution (100-300 μ L) with different compositions (Table 3.1), was poured into a round-bottom flask. Then, chloroform was evaporated by manually rotating the flask and using a dry nitrogen stream in a fume hood. The formed layer was left overnight +4 °C to ensure the removal of all solvent residues.

Table 3.1 : Different Lipid Solutions.

Lipid Composition	PC	PC:DGPE	PC:DGPE	PC:DGPE	PC:DGPE	DGPE
Molar Ratio	1	999:1	99:1	95:5	50:50	1

Hydration of lipid film

To hydrate the dried lipid film layer, 5-15 ml of 0.1 M phosphate buffered saline (PBS, pH 7.4) buffer was added to the flask, to obtain a final lipid concentration of 0.02 mg/ml. Then the flask was agitated vigorously for 10-15 min using a vortex.

Extrusion

Hydrated and vortexed lipid solutions initially form large, multilamellar vesicles. An extruder (Avanti Mini-Extruder) was, therefore, used to generate unilamellar liposomes. To do this, the obtained multilamellar liposomes were extruded with the help of two syringes 15 times through a 100 nm polycarbonate membrane (Figure 3.2). The obtained SUVs were collected in a falcon tube and stored at +4 °C overnight to be used on the following day. The syringes of extruder were washed by isopropanol and rinsed with abundant amounts of water. PTFE parts were cleaned by ethanol and stored in ethanol solution.

Due to the unstable nature of the liposomes, they were utilized within the 24 hours of preparation. Therefore, liposomes were produced freshly for each adsorption kinetic measurements.



Figure 3.2 : Liposomes were generated by an extruder

3.2.2 Imaging of liposomes with optical microscopy

A drop of multilamellar vesicle suspension obtained after vortex agitation was put on the coverslip and observed under 10x. The small unilamellar vesicles were also observed with 10x, 20x, 40x and 100x objectives, respectively with optical microscopy.

3.2.3 Measurement of adsorption kinetics

3.2.3.1 Preparation of gold surfaces

Immediately before each use, the surfaces of QCM crystal and SPR were cleaned by distilled water, and dried under nitrogen gas. After measuring the PC lipid vesicle adsorption onto the surface, the crystals were soaked in a mild detergent solution for several hours and then rinsed with water, dried under nitrogen, and stored. If thiolated lipid types (DGPE) were used in the experiments, a specific solution (5:1:1, $\text{H}_2\text{O}:\text{NH}_3(\%25):\text{H}_2\text{O}_2(\%30)$) was used to clean the thiol containing lipids from the gold surfaces and then the crystals were soaked in a mild detergent solution for several hours, rinsed with water, dried under nitrogen, and stored.

Oxidized gold surfaces

Oxidized gold surfaces were also utilized for some trials. For this purpose, the surfaces were oxidized with exposure to UV-ozone for 15 min, then rinsed with water, and dried under nitrogen.

3.2.3.2 Quartz crystal microbalance

Preparation of fluid chamber of QCM-D

QCM measurements were performed with QCM-Z500 (KSV Instruments) in a flow-through cell (Figure 3.3). The standard crystal sensor with 10 nm thickness gold coating has a fundamental frequency of 5 MHz and a diameter of 14 mm. The liquid flow through the cell was accomplished at $100\ \mu\text{L min}^{-1}$ by a peristaltic pump. All measurements were performed at $25\ ^\circ\text{C}$.

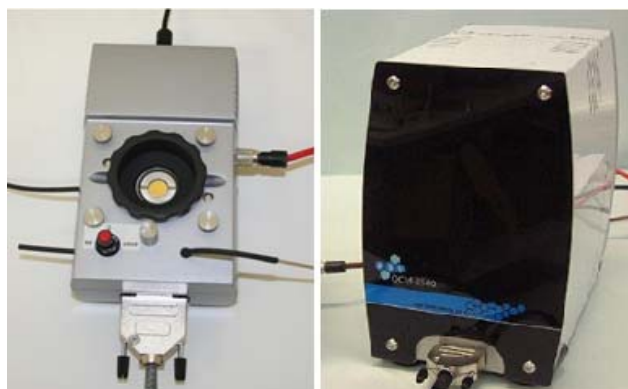


Figure 3.3 : The fully assembled QCM and the electronic unit.

Preparation of measurement cell of QCM-D

Before each experiment, the measurement cell of QCM and tubings were cleaned by passing through one volume of sodium dodecyl sulfate (SDS), one volume of ethyl alcohol and three volumes of distilled water. Then, the fluid cell was dried under nitrogen.

Crystals were then inserted into the measurement cell and the whole system is assembled (Figure 3.4). Clean tweezers were used when handling the o-ring and the crystal itself as these parts will be in direct contact with the sample.

Meanwhile, PBS was sonicated about 30-45 minutes to prevent the formation of bubbles which, otherwise, influence the QCM response in the magnitude of 1-2 Hz, and therefore leading to erratic results.



Figure 3.4 : The reassembly of the measurement cell.

Quartz Crystal Microbalance Measurements

Following the initiation of the system, PBS was firstly sent to the measurement cell. After the measurement system was tuned to the resonant frequency of the crystal, and a stable baseline was taken (generally after 15-20 min.), the buffer was replaced with one of the solutions of SUVs listed on Table 3.1. PBS was, then used to wash out the unadsorbed SUVs. All of the experiments were done at least three times with all type of SUVs.

The frequency (ΔF) and dissipation (ΔD) changes versus time were monitored by computer in real time at one fundamental and four overtone frequencies (15, 25, 35, 45, 55 MHz). These frequencies correlate with the third, fifth, seventh, ninth and eleventh harmonics ($n=3, 5, 7, 9, 11$). The frequency shifts were normalized to the fundamental frequency by division with the overtone number n .

3.2.3.3 Surface plasmon resonance spectroscopy

SPR measurements were performed with SR7000 Single Channel Surface Plasmon Resonance Spectrometer (Figure 3.5). Flow rate was adjusted by a peristaltic pump to $100 \mu\text{L min}^{-1}$. All measurements were performed at 25°C . Mass changes at the interface between the gold layer and the aqueous compartment caused changes in the local refractive index near the gold layer. The changes of refractive index were monitored by computer in real time.



Figure 3.5 : SR7000 Single Channel Surface Plasmon Resonance Spectrometer

Preparation of SPR set up

Before each run, SPR tubings were cleaned by passing through one volume of SDS, one volume of ethyl alcohol and three volumes of distilled water. SPR gold surface was cleaned with isopropanol and dried under nitrogen gas. After all parts of the set-up was cleaned, a drop of immersion oil was placed between the prizma and the slide surface and the whole measurement cell was assembled.

Sonication was used about 30-45 min. to remove dissolved gases from the PBS to prevent the SPR system from the air bubbles as in the case of QCM.

Surface Plasmon Resonance Spectroscopy Measurements

Firstly, PBS was sent to the setup till a stable baseline was obtained (generally after 5 min.), the buffer was then replaced with the solution of SUVs listed on Table 3.1. Then, PBS was pumped to the system to wash out the unadsorbed SUVs. All of the experiments were done at least three times with all type of SUVs.

4. RESULTS & DISCUSSION

4.1 Optical Microscopy of Liposomes

Hydrated and vortexed lipid solutions initially form “onion-like” (OLV), micron-scaled multilammellar vesicles (MLV) and these vesicles could be observed under 10x objective with optical microscopy (Figure 4.1). It was observed that their sizes vary between 2-6 μm diameter.

It could be seen in Figure 4.2 that these multilammellar vesicles were downsized to small unilammellar vesicles by the help of the extruder, which in turn were observed under 10x, 20x, 40x and 100x objectives, respectively. As it is seen, extrusion method yielded liposomes with diameter higher than 100 nm and smaller than $\sim 1 \mu\text{m}$ like it had been reported in literature [15].

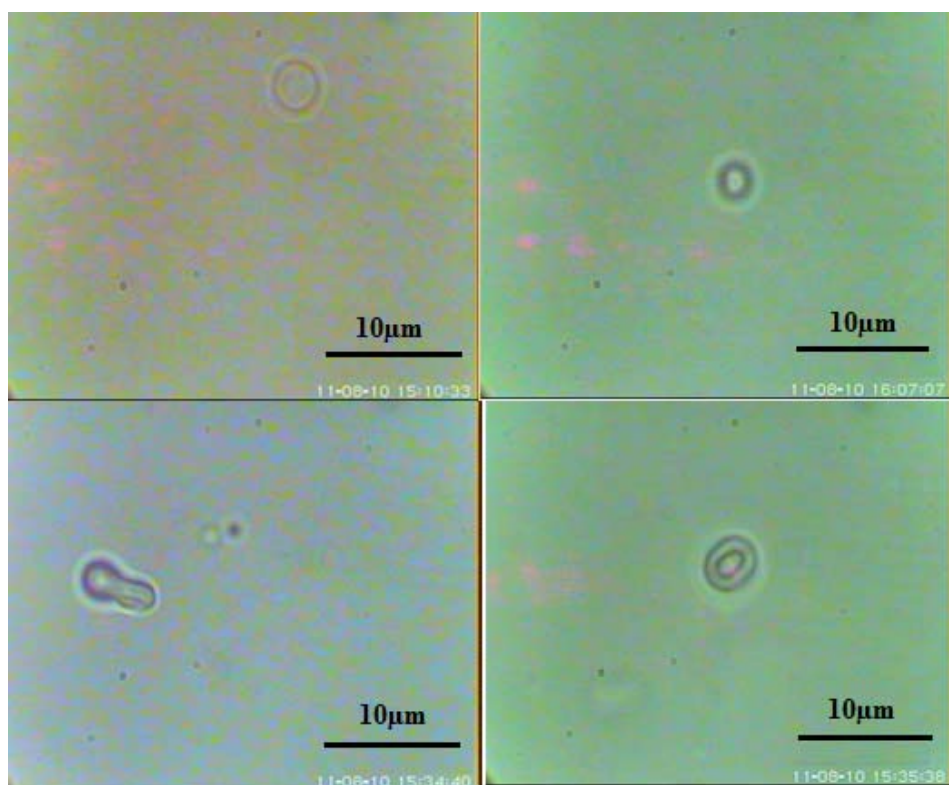


Figure 4.1 : Multilammellar vesicles observed under 10x objective.

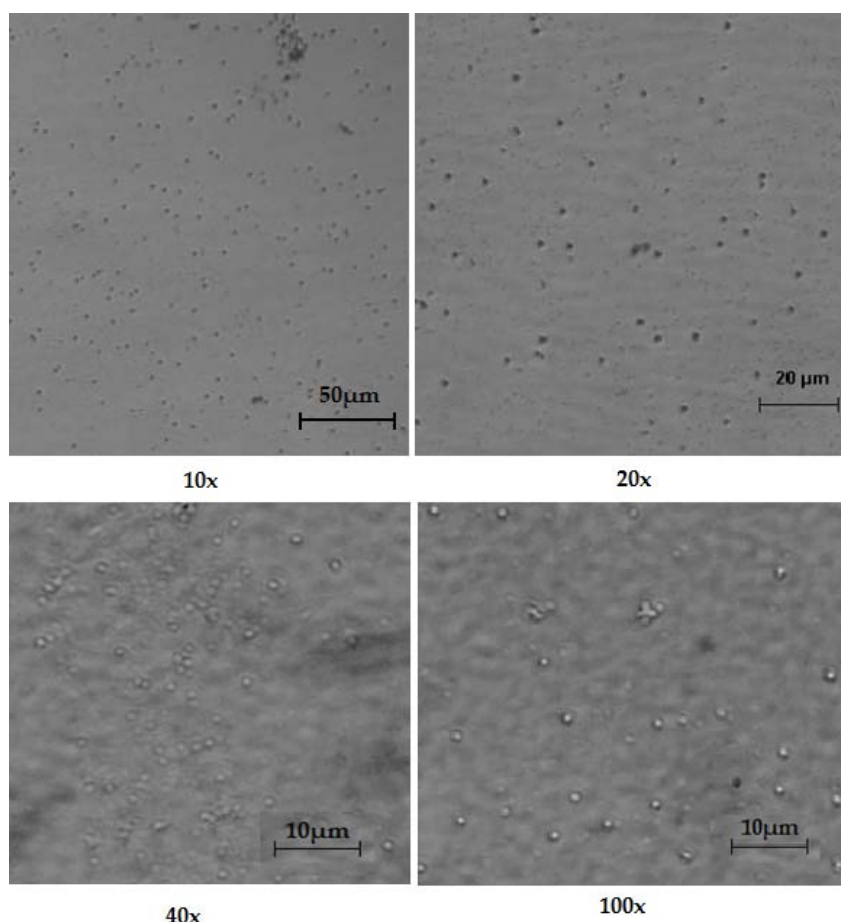


Figure 4.2 : Small unilamellar vesicles observed under 10x, 20x, 40x and 100x objectives, respectively

4.2 Interaction of PC Liposomes with Gold Surface

The frequency (Δf) and dissipation change (ΔD) data with different harmonics were obtained separately with the software of the QCM device. However, to see the results as a whole, all of the figures for QCM results were displayed as the measured normalized frequency and dissipation shifts as a function of time for each experiment. Complementary SPR results were also given.

Transient spikes encountered were originated from the buffer to buffer or buffer to sample exchange. The transient recovered within a few seconds and did not affect the baseline of the measurement.

4.2.1 Unoxidized surfaces

Many authors concluded that the most important factors that determine the destiny of intact liposomes upon adsorption are the surface charge and the lipid composition

[49]. Therefore, liposome behaviour was firstly tested according to the charge of the gold surface.

It could be seen from the Figure 4.3 and Figure 4.4 that PC liposomes did not interact with the unoxidized gold surfaces. There was no change in frequency and dissipation in QCM-D and in refractive index in SPR. This result was expected when the zwitterionic structure of PC was considered (Figure 2.1). Because, gold, when not oxidized, is poorly hydrophilic, and have a low surface charge, which is not adequate to support intact liposomes of zwitterionic lipids [47].

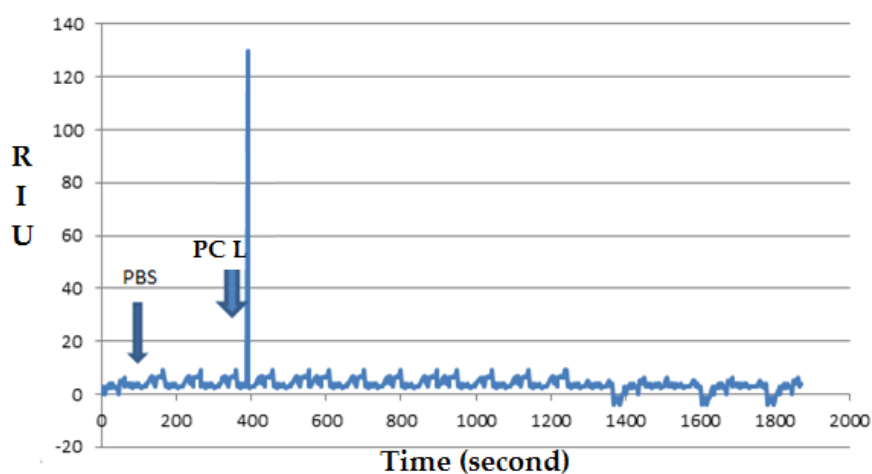


Figure 4.3 : Change in refractive index unit (RIU) versus time for the interaction of PC liposomes onto an unoxidized gold.

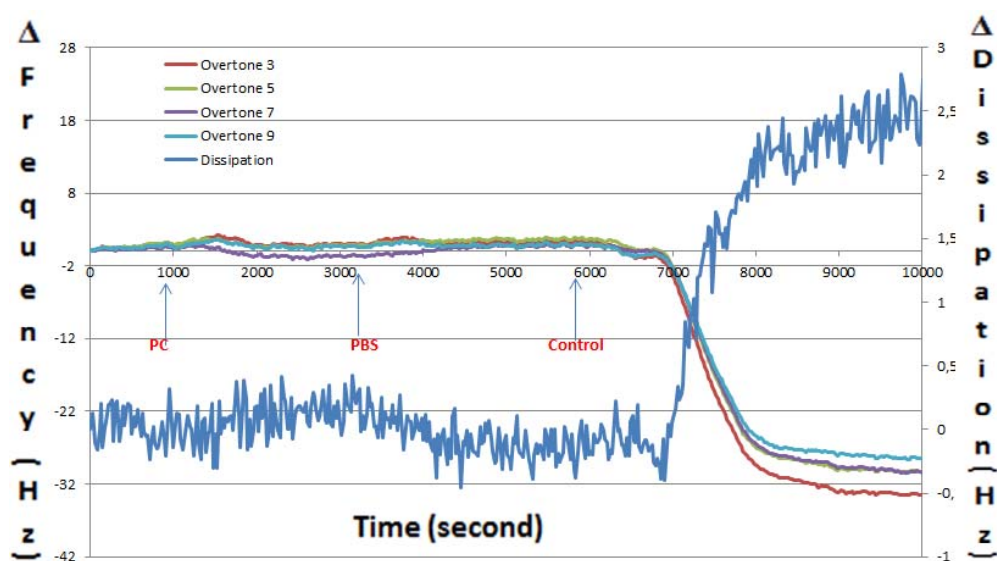


Figure 4.4 : Change in QCM resonant (normalized) frequency and dissipation versus time for the interaction of PC liposomes onto an unoxidized gold.

To see the effect of a molecule that can interact with gold surface, another type of lipid molecule (DSPE-PEG) were used in QCM as a control parameter. It was found that DSPE-PEG interacted with the unoxidized gold surfaces. It is known from the literature that, the polymeric chains of polyethylene glycol (PEG) are adsorbed physically onto the gold [46].

4.2.2 Oxidized surfaces

When the adsorption behavior of PC SUVs onto oxidized gold surface was investigated, change in the refractive index was observed (Figure 4.5). This finding could be attributed to the intact adsorption of close-packed layer of lipid vesicles on SPR surface that was also observed in previous studies [4]. The adsorption saturated at a value that was unaffected by rinsing. The binding process, which corresponds to an increase about 800 RIU, was complete within 35 minutes.

Oxidation increased the polarizability of the gold surface and that possibly provided the attractive potential, which makes vesicles to adhere more easily to the surface as commented in literature [2].

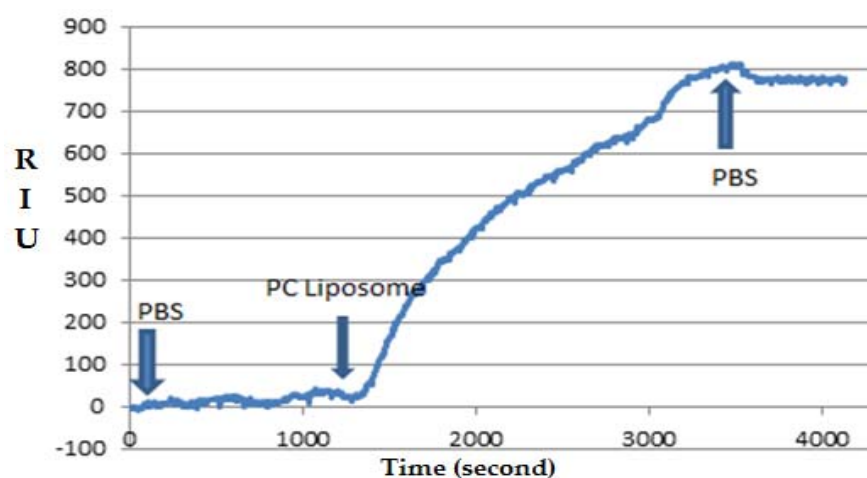


Figure 4.5 : Change in refractive index unit (RIU) versus time for the interaction of PC liposomes onto an oxidized gold.

When the QCM-D results were examined, it was seen that there was a shift in the resonant frequency accompanied by a change in the dissipation, but it was affected by PBS rinsing (Figure 4.6). Hence, it could be suggested that there was an adsorption of intact lipid vesicles, but they had not formed a closely packed layer on the surface.

The low frequency and dissipation shift (~ 5 Hz, $\sim 0.2 \cdot 10^{-6}$ Hz, $\Delta D/\Delta f = 0.04$) also not correspond to that expected [2] adsorption of closely packed lipid vesicles. This difference might be the result of the different flow direction of the fluid onto the measurement chambers in SPR and QCM-D. In SPR, the arrival of the fluid onto the surface was from the top and gravity force might be contributing to the electrostatic interaction between gold and the liposomes. However, parallel flow cell of QCM-D device does not support the feed of gravity. Beside, the other ground might be the fact that the active interaction area of QCM-D slide (78.5 mm^2) is broader than of SPR (16 mm^2).

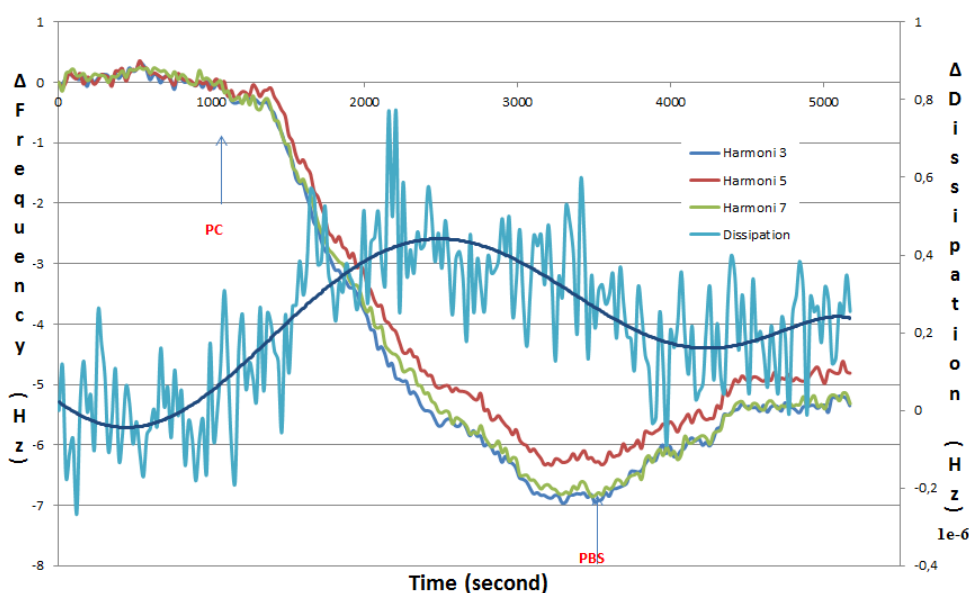


Figure 4.6 : Change in QCM resonant (normalized) frequency and dissipation versus time for the interaction of PC liposomes onto an oxidized gold.

4.2.2.1 Effect of the liposome concentration

When the concentration of lipids for liposome preparation was doubled (0.04 mg/ml), it was observed that the frequency and dissipation shift increased (~ 7 Hz, $\sim 0.9 \cdot 10^{-6}$ Hz, $\Delta D/\Delta f = 0.13 \pm 0.1$) as expected (Figure 4.7). At this point, it is practical to evaluate the $\Delta D/\Delta f$ ratio to compare the different outcomes since it is a critical parameter to derive conclusive information about liposomal behavior during the binding process [44]. In that case, the increase at the $\Delta D/\Delta f$ ratio compared with former situation (Figure 4.6) indicating the increment of $\Delta \text{total volume} / \Delta \text{total surface area}$ of the liposomes. When new vesicles adsorb to the surface, a large amount of water trapped within the intact vesicles as well as between vesicles adsorbed onto the surface [4]. Therefore, the viscoelasticity of the vesicle layer increased. This trapped

water is able to dissipate a large amount of energy unlike the water that rests on top of a bilayer [26].

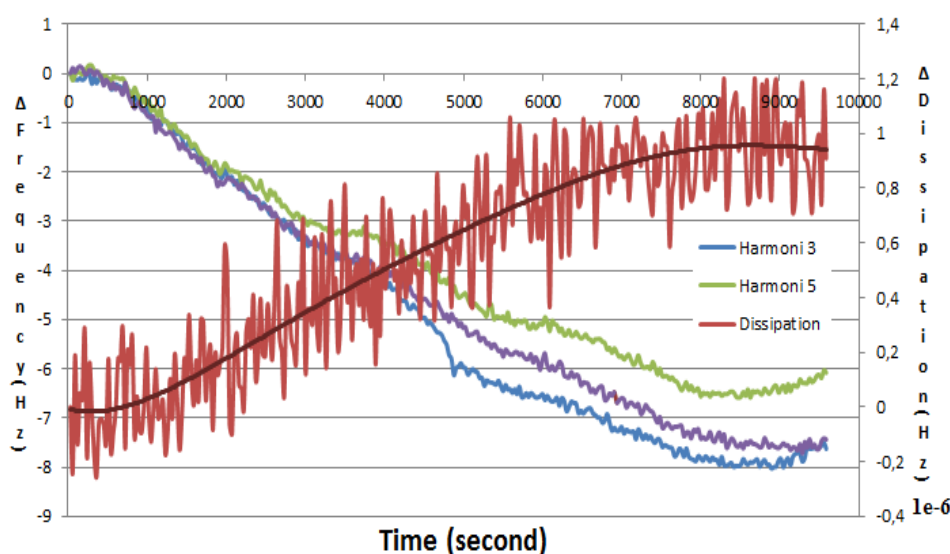


Figure 4.7 : Change in QCM resonant (normalized) frequency and dissipation versus time for the interaction of PC liposomes (2x concentration of lipids) onto an oxidized gold.

4.2.2.2 Effect of the oxidation time

When the oxidation duration of the gold surface was doubled (30 min.), $\Delta D/\Delta f$ value increased ($\Delta f \sim 6$ Hz, $\Delta D \sim 0.9 \times 10^{-6}$ Hz, $\Delta D/\Delta f = 0.16 \pm 0.02$) as anticipated (Figure 4.8).

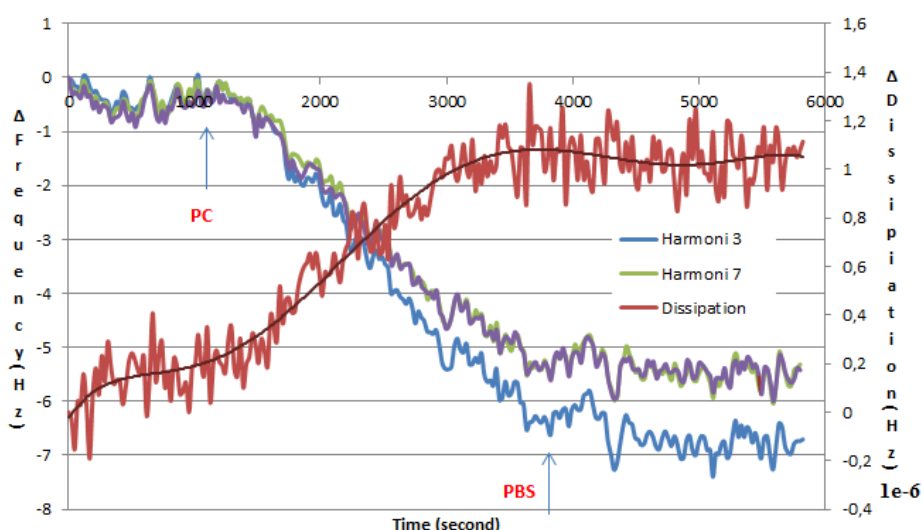


Figure 4.8 : Change in QCM resonant (normalized) frequency and dissipation versus time for the interaction of PC liposomes onto a 30' oxidized gold.

The increase at the $\Delta D/\Delta f$ ratio compared with 15 min oxidation time indicated the increased number of the liposomes adhered to the highly polarized gold surface leading to the increased softness of the vesicle layer.

4.2.2.3 Comparison of the single pass system with the recycled one

The experiments were generally carried out in a single pass system in which different molecules were gotten into contact with the surface only once. When the exit stream from the measurement chamber was recycled back to the system it was possible to obtain an incubation with the same solution for a long periods of time, in this case for 18 hours. Recycling the solution was thought to saturate the gold surface with more liposomes over time. It was seen that $\Delta D/\Delta f$ value increased 7-8 times ($\Delta f \sim 20$ Hz, $\Delta D \sim 6.4 \times 10^{-6}$ Hz, $\Delta D/\Delta f = 0.3 \pm 0.03$) as expected (Figure 4.9).

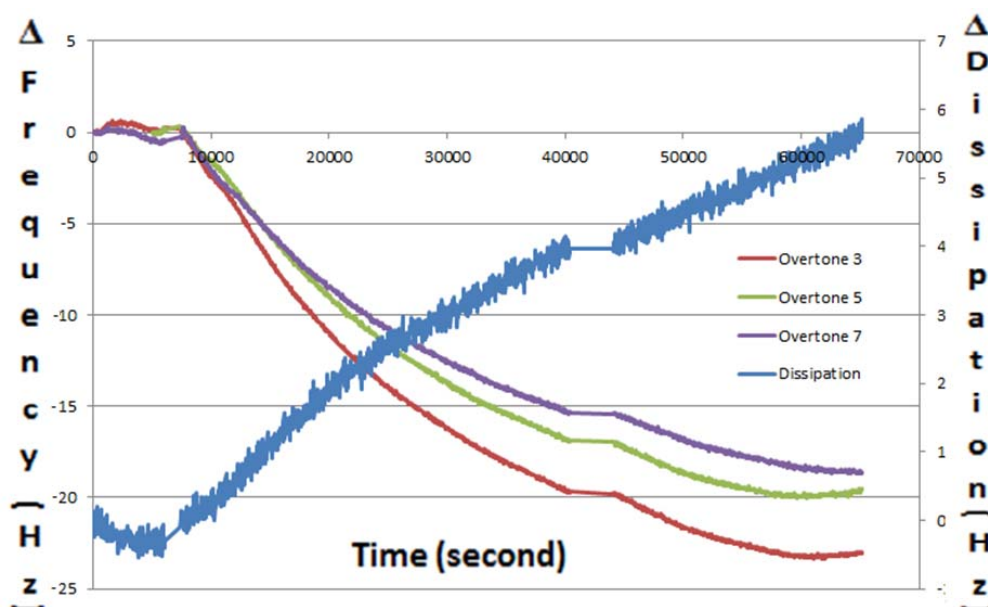


Figure 4.9 : Change in QCM resonant (normalized) frequency and dissipation versus time for the interaction of PC liposomes onto oxidized gold in recycled system.

It had been reported that when the $\Delta f/n$ curves relative to the different overtones overlap and the dissipation change is small, the film is rigid. In contrast, if the $\Delta f/n$ curves are shifted and dissipation change is high, the film is not rigid [47]. Therefore, in that case, the separation between frequency overtones observed shows the dramatic increase at the softness. This could be attributed to the intact adsorption of closely packed layer of lipid vesicles on the surface [2]. The prolonged adsorption process saturated the surface at a value that was unaffected from rinsing.

It was seen from the results that the high adsorption capacity of the oxidized gold surface was the driving force that enables vesicles to remain intact and stable on the gold support (Figure 4.10) [31]. However, this strong attractive potential did not cause the vesicles to rupture to form a bilayer as could be seen from the high $\Delta D/\Delta f$ values (Figure 4.7-4.9). Summary of the experimental values obtained from QCM-D for PC liposomes were listed in the Table 4.1.

The stability of the liposomes on the surface was also tested. The values of Δf and ΔD stabilized and remained constant for at least 1.5-2 h, suggesting that the immobilized liposomes maintained their three-dimensional configuration.

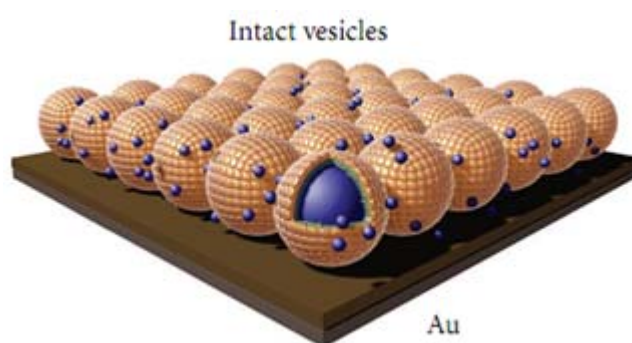


Figure 4.10 : Vesicles remain intact and stable on the oxidized gold support.

It could be seen that immobilizing liposomes on oxidized gold is a simple method to form stable monolayers of intact liposomes. These monolayers can be used as three-dimensional membrane models in future studies of drug–lipid interactions [47].

Table 4.1 : Summary of the experimental values with PC liposomes.

Liposome	Concentration	UV-Ozone (min.)	$\Delta D/\Delta f_n$ (*1e-6)
PC	1x	-	0
PC	1x	15'	0.04±0.01
PC	2x	15'	0.13±0.01
PC	1x	30'	0.16±0.02
PC (cycle)	1x	15'	0.30±0.03

4.3 Interaction of PC-DGPE Liposomes with Gold Surface

In order to construct lipid bilayers on the gold surfaces, the general approach was first to modify the gold surfaces with some molecules, especially with the ones that could form self-assembled monolayers (SAMs) [26]. The attachment of these

molecules were commonly realized through the chemical covalent coupling of thiol groups with Au and hence, a chemically and mechanically robust attachment of anchor lipids to the solid support were done [50]. In this thesis, an alternative method was tried by incorporating thiol-terminated lipids (DGPE) to PC at different ratios as listed in Table 3.1 and by bringing these liposomes into contact with gold surfaces.

4.3.1 Adsorption of 0,1 % DGPE–PC liposomes

It could be seen from the Figure 4.11 that DGPE–PC liposomes interacted with the unoxidized gold surfaces strongly and rapidly when compared with PC (Figure 4.5). The binding process, which corresponds to an increase about 1600 RIU, was completed within 20 minutes. The result was reasonable since the thiol groups in DGPE structure (Figure 3.1) have strong interactions with gold surfaces [48].

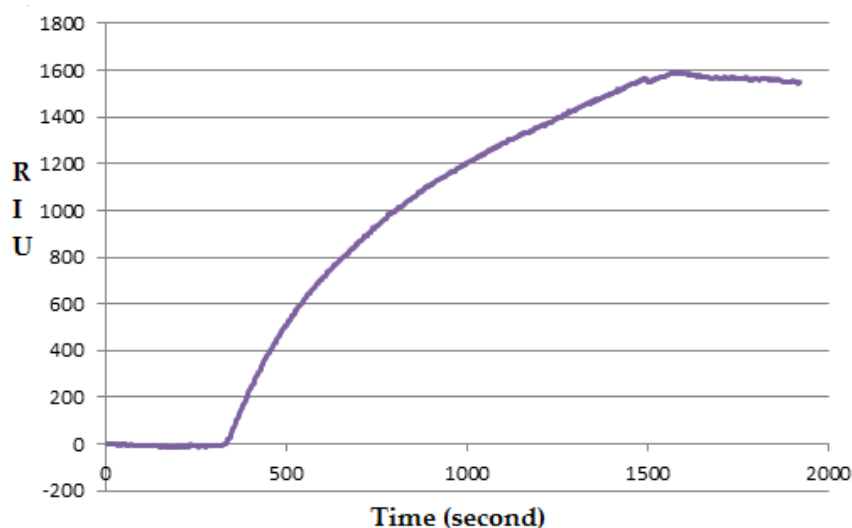


Figure 4.11 : Change in refractive index unit (RIU) versus time for the interaction of 0,1 % DGPE–PC liposomes onto unoxidized gold.

Figure 4.12 and 4.13 shows QCM-D data for 0,1 % DGPE–PC liposomes ($\Delta f \sim 11$ Hz, $\Delta D \sim 0.7 \cdot 10^{-6}$ Hz, $\Delta D/\Delta f = 0.06 \pm 0.01$) and 2 % bovine serum albumin (BSA) ($\Delta f \sim 18$ Hz, $\Delta D \sim 0.8 \cdot 10^{-6}$ Hz, $\Delta D/\Delta f = 0.04 \pm 0.00$).

It is known that a high viscoelasticity of bound analytes induces an increase in damping frequency hence, a differentiation of intact liposomes from a fused bilayer formation is possible through the ratio of damping and frequency change [34, 44]. In this case, $\Delta D/\Delta f$ value was considerably decreased by the addition of DGPE to PC liposomes (from 0.30 to ca. 0.06).

The low $\Delta D/\Delta f$ value (0.06 ± 0.00) for liposomes containing thiol-terminated lipids suggested the rupture of the liposomes and formation of a lipid bilayer (Figure 4.14). This suggestion was based on the $\Delta D/\Delta f$ value (0.04 ± 0.00) of an adsorbed BSA, which was used as a reference for a rigid monolayer [44] on the surface. The frequency overtones overlapped also indicated the formation of a rigid layer.

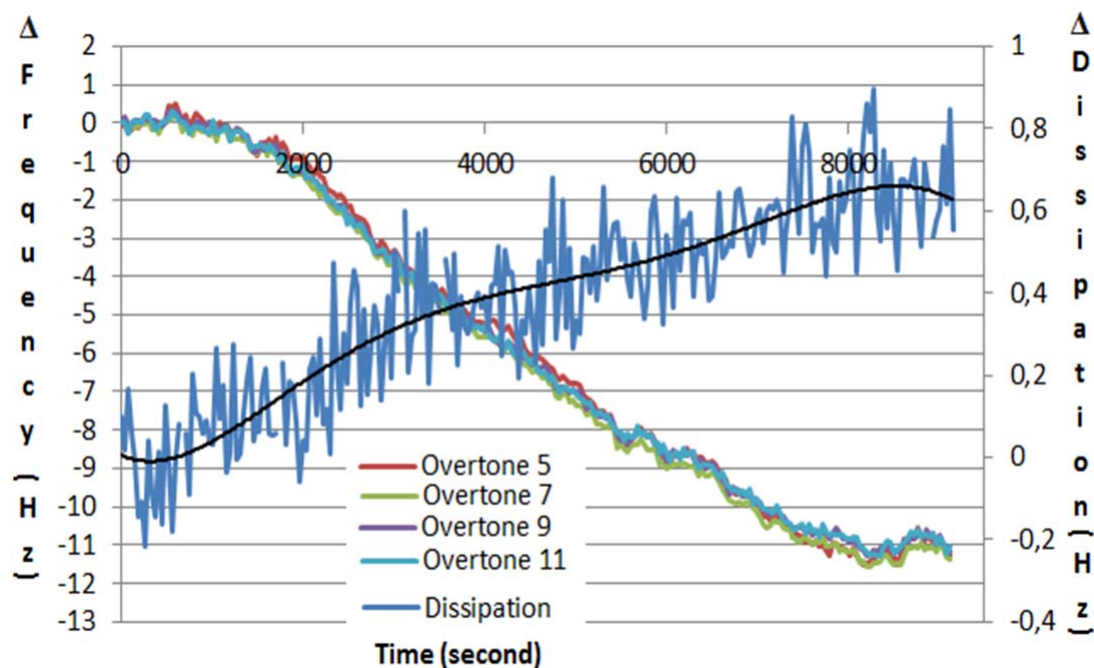


Figure 4.12 : Change in QCM resonant (normalized) frequency and dissipation versus time for the adsorption of 0,1 % DGPE-PC liposomes unoxidized onto gold.

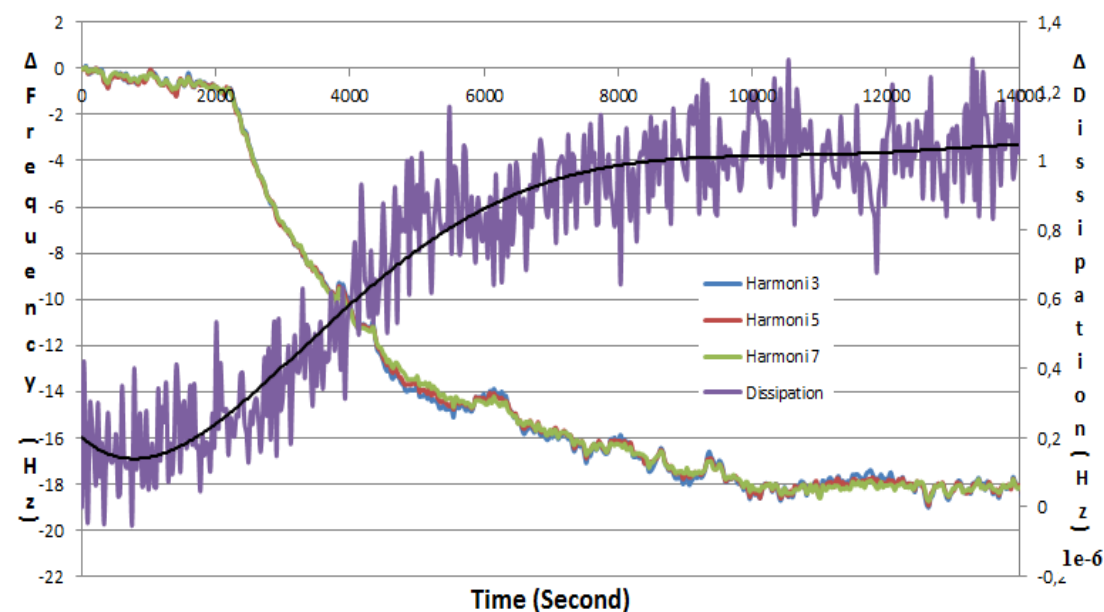


Figure 4.13 : Change in QCM resonant (normalized) frequency and dissipation versus time for the interaction of 2 % BSA with unoxidized gold.

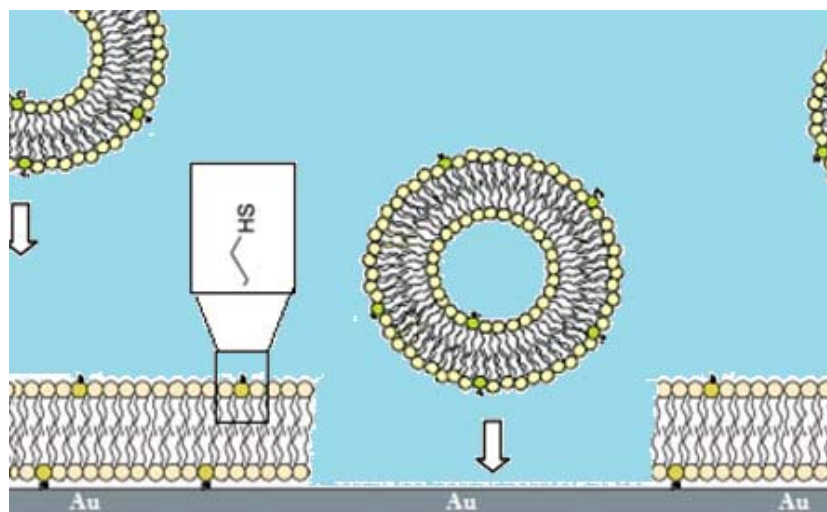


Figure 4.14 : The rupture of the thiolated liposomes and formation of a lipid bilayer on unoxidized gold (thiol group ratio is not to scale).

4.3.2 Adsorption of 1, 5, 50 % DGPE–PC and DGPE liposomes

It can be seen from Figure 4.15 that the adsorption rate of the liposomes and the mass on the surface was increased parallelly with the increase in the DGPE lipids ratio of the liposomes. The binding process, which corresponds to an increase about 1600-4000 RIU, was complete within 6-7 minutes.

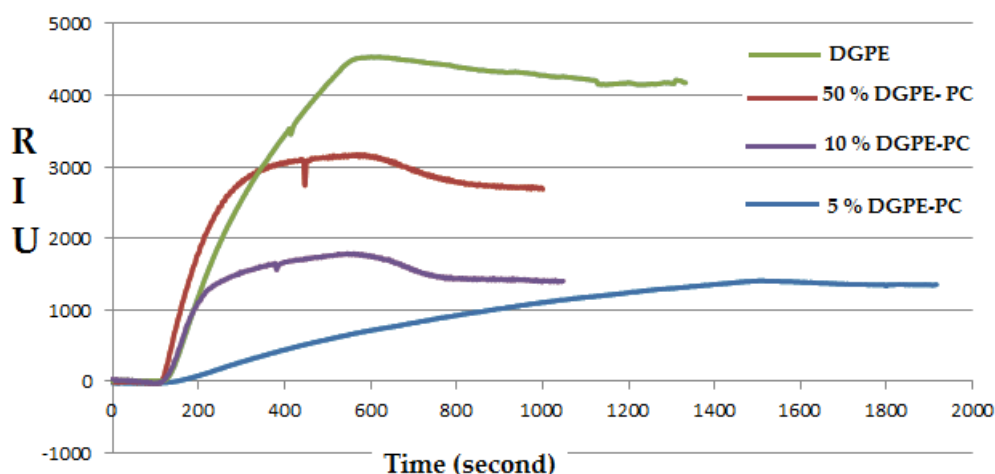


Figure 4.15 : Change in refractive index unit (RIU) versus time for the interaction of 5, 10, 50 % DGPE–PC and DGPE liposomes onto unoxidized gold.

Figures 4.16-17 show QCM-D data for 1 and 5 % DGPE–PC liposomes. Adsorption of 1 % DGPE-PC liposomes resulted in Δf value of $\sim 36 \pm 3$ Hz, $\Delta D \sim 3.5 \times 10^{-6}$ Hz and $\Delta D/\Delta f = 0.10 \pm 0.01$. Increasing the DGPE lipid ratio from 1 % to 5 % increased Δf ($\sim 54 \pm 8$ Hz) and ΔD ($\sim 4.3 \times 10^{-6}$ Hz) values, but $\Delta D/\Delta f$ value was decreased (0.08 ± 0.01) slightly.

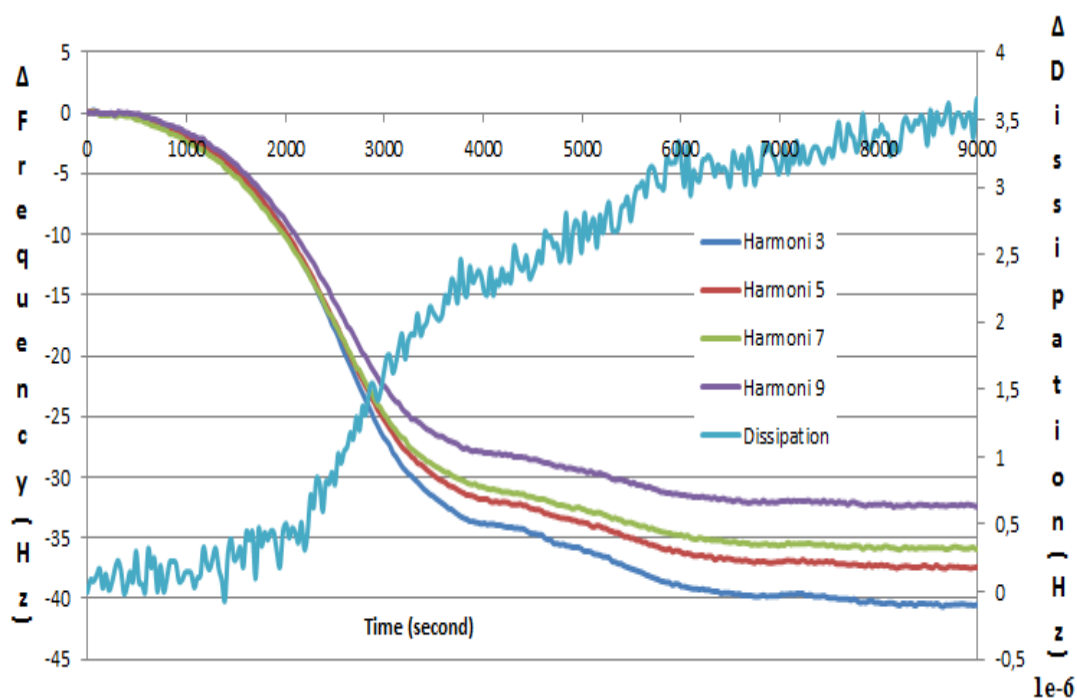


Figure 4.16 : Change in QCM resonant (normalized) frequency and dissipation versus time for the adsorption of 1 % DGPE-PC liposomes onto unoxidized gold.

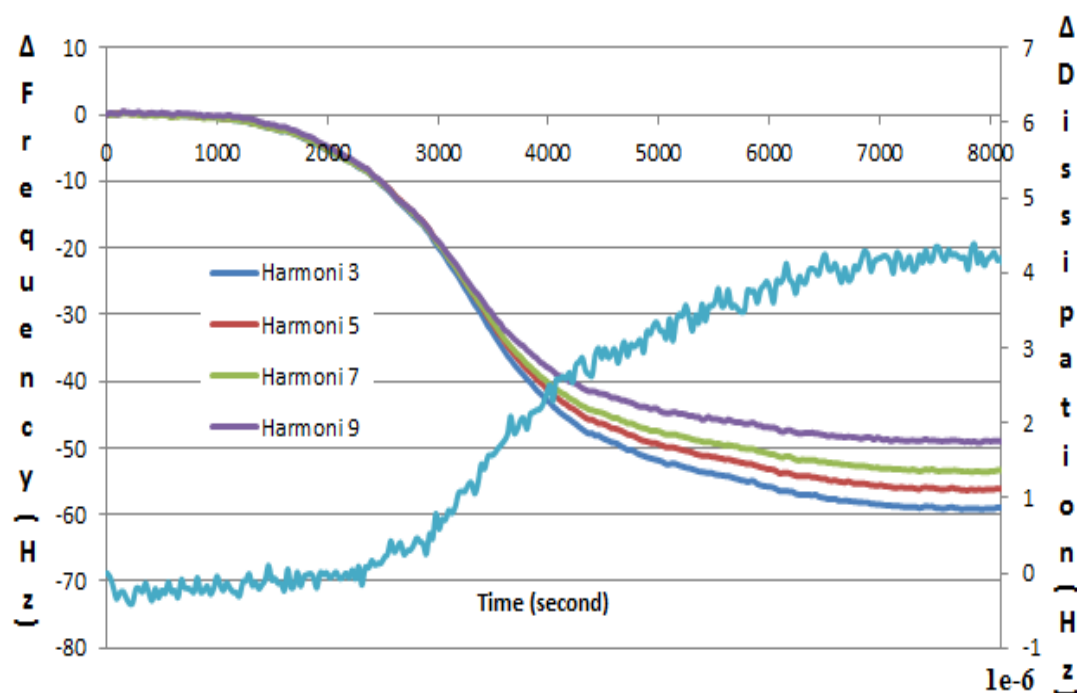


Figure 4.17 : Change in QCM resonant (normalized) frequency and dissipation versus time for the adsorption of 5 % DGPE-PC liposomes unoxidized onto gold.

Adsorption of 50 % DGPE-PC liposomes resulted in the values of $\Delta f \sim 74 \pm 9$ Hz, $\Delta D \sim 7 \times 10^{-6}$ Hz and $\Delta D/\Delta f = 0.09 \pm 0.01$. Using only DGPE was shown to slightly decrease

Δf ($\sim 63 \pm 8$ Hz) and ΔD ($\sim 5.4 \times 10^{-6}$ Hz) values without affecting the $\Delta D/\Delta f$ ratio (0.08 ± 0.01).

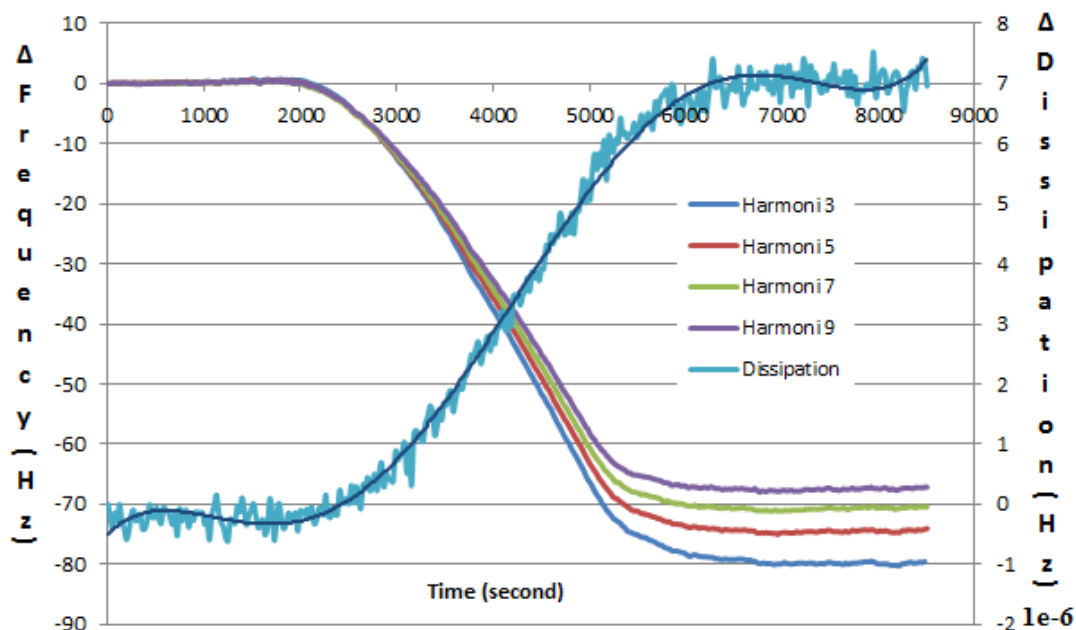


Figure 4.18 : Change in QCM resonant (normalized) frequency and dissipation versus time for the adsorption of 50 % DGPE-PC liposomes onto unoxidized gold.

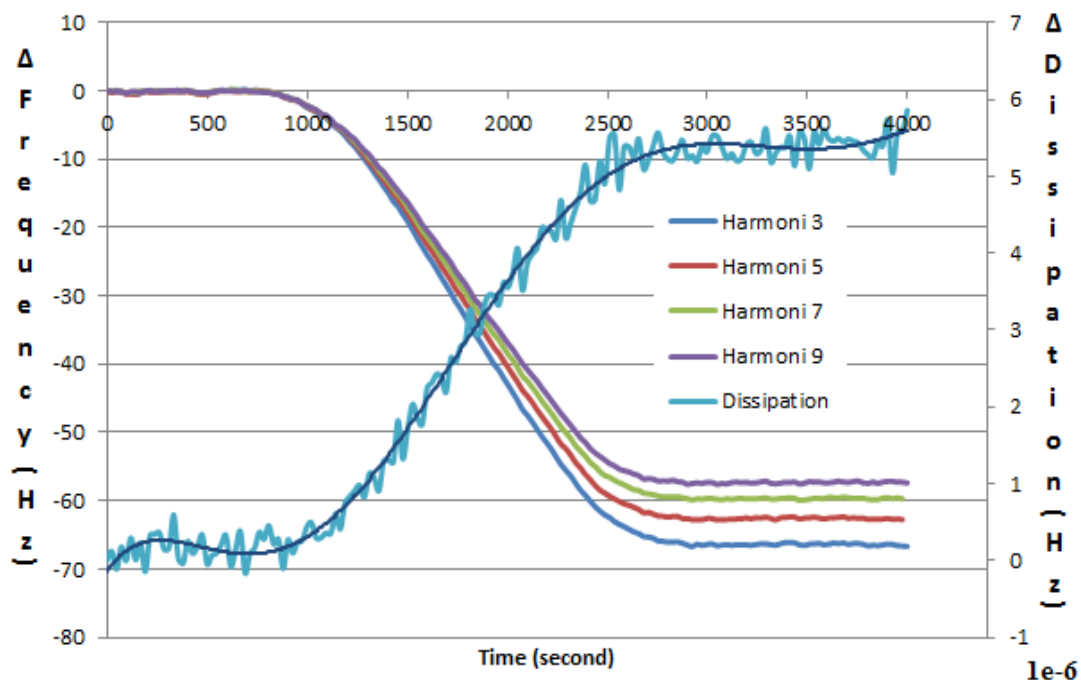


Figure 4.19 : Change in QCM resonant (normalized) frequency and dissipation versus time for the adsorption of DGPE liposomes onto gold.

Summary of the experimental values obtained from QCM-D for 1, 5, 50 % DGPE-PC and 100 % DGPE liposomes are listed in the Table 4.2.

The increase in the Δf_n values show increased mass on the surface. This is probably the indication of multilayer formation at high DGPE lipid concentrations (1-100 %). This finding was expected because of the strong interactions between thiol-thiol groups and thiol-gold surface (Figure 4.20).

Table 4.2: Summary of the experimental values with DGPE-PC and DGPE liposomes and BSA % 2.

Solution	ΔD ($1e-6$ Hz)	Δf_n (Hz)	$\Delta D/\Delta f_n$ ($*1e-6$)
2 % BSA	0.8	18\pm0	0.04\pm0.00
0,1 % DGPE - PC	0.7	11\pm0	0.06\pm0.00
1 % DGPE – PC	3.5	36\pm3	0.10\pm0.01
5 % DGPE – PC	4.3	54\pm8	0.08\pm0.01
50 % DGPE - PC	7.0	74\pm9	0.09\pm0.01
DGPE	5.4	63\pm8	0.08\pm0.01

When the DGPE lipid ratio was increased, the mass accumulated on the surface increased correspondingly and the duration of mass/multilayer formation decreased on the surface. This observation was more apparent at 50 % DGPE-PC and DGPE liposomes (Figures 4.18-19). Because, the more ratio of thiol groups within the liposome, the more rapid interaction would be with each other and the surface. This finding was also confirmed with the SPR data (Figure 4.15).

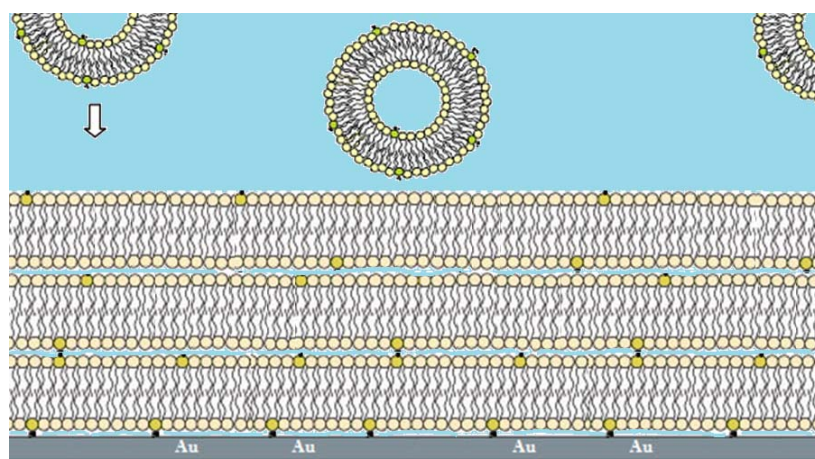


Figure 4.20 : The formation of multilayers and the entrapped water between the layers (not to scale).

In addition, for 1-100 % DGPE lipid ratios, it was observed that, after a certain period of time, a separation was occurred among the frequency overtones. This could also be considered as a proof of the formation of a rigid bilayer first and then a continuous build-up of rigid and compact phospholipid multilayers with little

entrapped water between the layers. On the contrary of the high DGPE containing liposomes, there was not any overtone separation for 0.1 % DGPE-PC ones.

The values of Δf and ΔD stabilized and remained constant for at least 1 h, indicating the stability of the layers.

It could be concluded that there was slight differences between DGPE-PC (1-100 %) and DGPE liposomes, except the formation speed of the multilayer and the layer number. A slightly higher value of $\Delta D/\Delta f$ of 1 % DGPE-PC liposomes (0.10 ± 0.01) compared to 5, 50 % DGPE-PC and DGPE liposomes could be a result of less or not deformed or flattened liposomal structures on the bilayer/multilayer surface due to the relatively low thiol groups to the others.

4.4 The Effect of Na^+ and Ca^{++} Ions on the Multilayers

Since there are lots of application areas of supported lipid layers that the ionic strength of the solution is crucial, it is important to see the effects of the ionic solutions on lipids. That's why, QCM-D and SPR were also used to evaluate the effects created by a divalent cation, CaCl_2 and a monovalent cation, NaCl in DGPE-PC multilayers that were composed of zwitterionic lipids.

Figure 4.21 shows the SPR data showing the effect of Ca^{++} ions on the multilayers. It is obvious that there is a significant increase in the signal even after PBS rinsing.

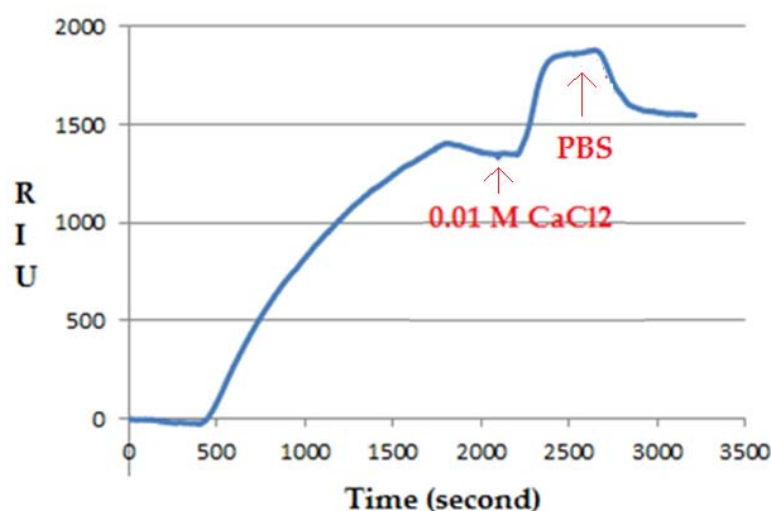


Figure 4.21: Change in refractive index unit (RIU) versus time for the effect of 0.01M Ca^{++} ions on the multilayers.

Figures 4.22-24 shows that, exposing the multilayer to Ca^{++} for 15-20 min. firstly caused a slight loss of mass in the QCM measurement. It is reported for divalent cations that they bind to the phosphate group of the phospholipids and form Ca^{++} -PC complexes. It has also been shown that in some surface-vesicle combinations, which tend not to form SLBs in the most common buffer solutions, SLBs formation can be promoted by adding Ca^{++} ions [51]. Hence, it is reasonable to conclude according to the literature that residual (flattened or less deformed) vesicles on the multilayers were ruptured entirely by Ca^{++} and consequently the entrapped buffer was released resulting in the loss of mass. But this observation was not seen in SPR data, and this could be originated from the different conditions between SPR and QCM-D. It could be thought that there was not residual vesicles left on the multilayer in SPR gold surface, but in QCM-D.

Then, an increase in dissipation is observed. The increased dissipation change indicates that there was an increase in viscosity of the adsorbed film. Further evidence of increased viscosity is indicated by the separation of each harmonics (15, 25, 35, 45 MHz) (Figure 4.22).

The effect of Ca^{++} ions could be seen clearly when the molar ratio was increased (Figure 4.23-24).

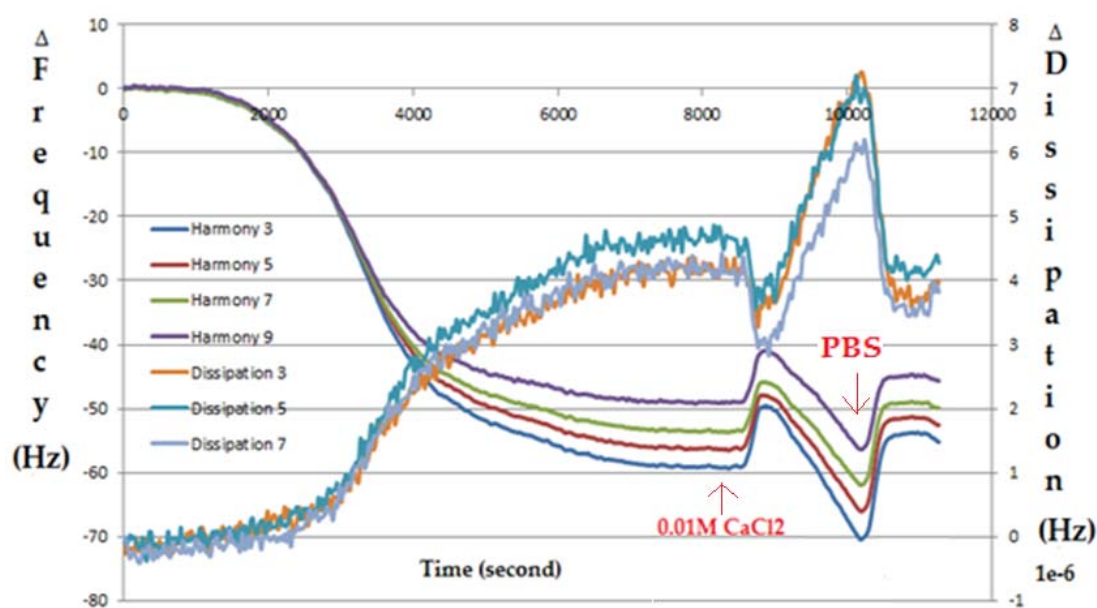


Figure 4.22 : Change in QCM resonant (normalized) frequency and dissipation versus time for the effect of 0.01M Ca^{++} ions on the multilayers

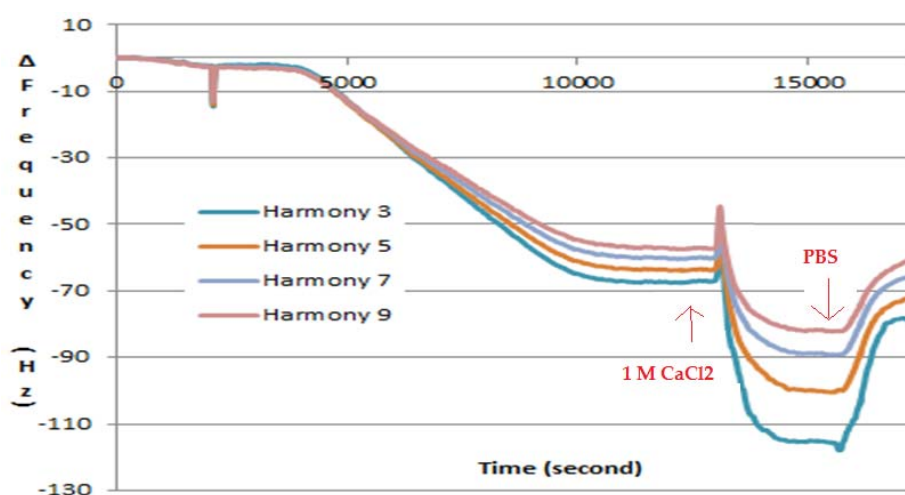


Figure 4.23 : Change in QCM resonant frequency versus time for the effect of 1 M Ca^{++} ions on the multilayers.

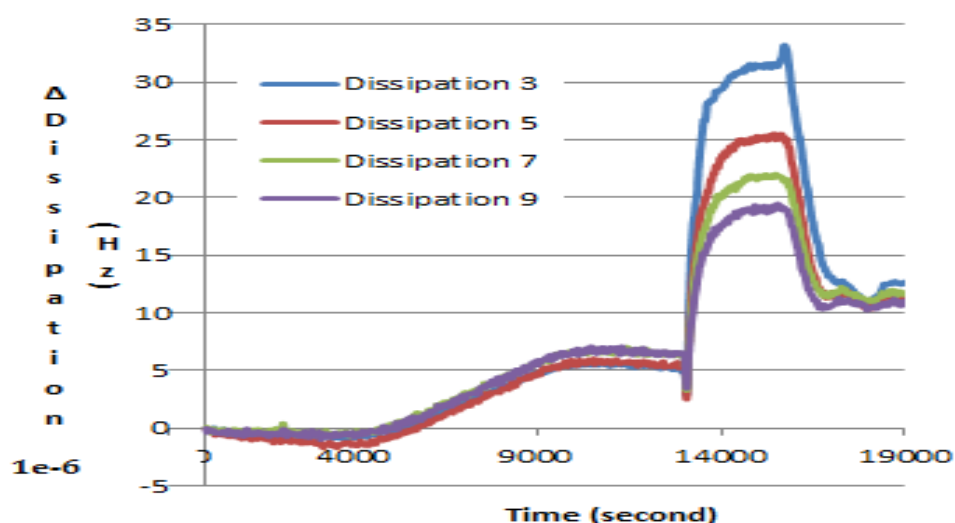


Figure 4.24 : Change in QCM dissipation versus time for the effect of 1 M Ca^{++} ions on the multilayers.

Seeing the dramatic increase of $\Delta D/\Delta f$ value after Ca^{++} flow, it could be suggested that the multilayers were solubilized with Ca^{++} and local disruptions might occurred, so the softer regions were formed where water was possibly entrapped again and result in as mass increase also. Looking at the separation of dissipation changes also, for each harmonics actually indicates that the layers deposited are not so well connected to the surface of the quartz crystal after Ca^{++} flow. An understanding of the mechanism of membrane disruption caused by Ca^{++} is possible when seeing the fact that divalent ions could modify the electrostatic interactions or directly interact with lipids [45, 51]. Additionally, it could be assumed that presence of Ca^{++} ions

between the gold surface and lipid layer and the interactions with phospholipid headgroups in that layer might have substantial effects on the deposition and so viscoelastic properties of the lipid layers.

Lastly, the monovalent cation, Na^+ ions exhibited a much weaker but similar effect as Ca^{++} ions (Figure 4.25) that was an expected result since calcium ions interact more strongly with phospholipids, than sodium ions [52].

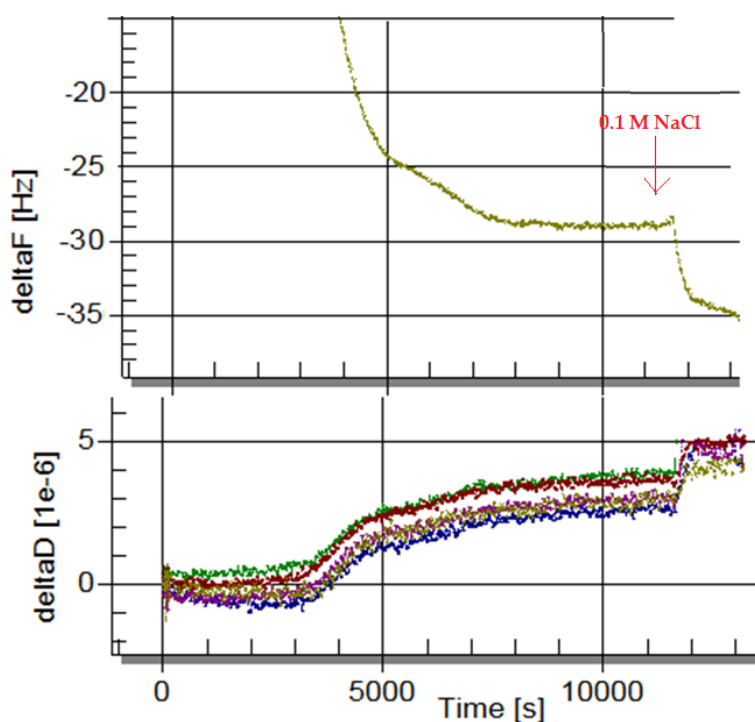


Figure 4.25 : Change in QCM frequency and dissipation versus time for the effect of 0.1 M Na^+ ions on the multilayers.

5. CONCLUSIONS & FUTURE WORKS

Lipid bilayers on solid supports are important model membrane systems to mimic the biological membranes and their constituents. Because of the complexity of biomembranes, there is a clear need to develop new model membrane systems to study one or a few membrane components. In this study, the effect of thiolated lipids on the construction of lipid bilayers evaluated with QCM-D and SPR. QCM-D and SPR are important tools that can give detailed informations about adsorption events on surfaces, therefore the properties of the resulting lipid layers in real-time using frequency-dissipation changes (Δf - ΔD) and refractive index shift, respectively. In addition, the $\Delta D/\Delta f$ ratio obtained in QCM-D provides information about the viscoelastic behavior of the constructed layer, thus gives valuable insights about the binding process.

PC liposomes recycled in the system, which did not contain any thiol group, formed a layer onto the oxidized gold surface. The layer remained stable for at least 1.5-2 h, suggesting the immobilization of vesicles. These vesicle monolayers could be used as three-dimensional membrane models in future studies. On the other hand, these vesicles were rapidly washed from unoxidized surfaces.

DGPE containing vesicles could interact with unoxidized gold surfaces due to their thiol groups. Even at low DGPE-PC ratio (0,1 %), the findings suggested the rupture of the liposomes and formation of a lipid bilayer. Moreover, DGPE lipid concentrations higher than 1 % indicated the build-up of rigid and compact phospholipid multilayers with low entrapped water content.

The effect of Na^+ and Ca^{++} ions on DGPE-PC multilayers were also evaluated. It was seen that 0.01 M Ca^{++} solubilized and/or disrupted the multilayers and Na^+ ions exhibited a much weaker but similar effect. Hence, it could be said that electrostatic interactions between lipid-buffer interface control structural and dynamic properties of lipid layer which is especially important when model membranes are used as immobilization surfaces for an enzyme, protein, etc.

In conclusion, an alternative way to construct lipid bilayer/multilayer structures on the gold surfaces was suggested through incorporating thiol-terminated lipids to PC at different ratios.

As a future work, different layers will be characterized by liquid Atomic Force Microscopy and the interactions of bilayers with cells will be explored.

REFERENCES

- [1] **Richter, R. P., Him, J. L. and Brisson, A.** (2003). Supported Lipid membranes, *Materials Today*, Laboratory of Molecular Imaging and NanoBioTechnology, IECB, CNRS-UMR 5471.
- [2] **Keller, C. A.; Kasemo, B.** (1998). Surface Specific Kinetics of Lipid Vesicle Adsorption Measured with a Quartz Crystal Microbalance. *B. Biophys. J.*, 75, 1397–1402.
- [3] **Volker, K., Marta K., D., David, M., Chen, W. and Lukas K., T.** (2008). Supported Lipid Bilayers: Development and Applications in Chemical Biology, *Wiley Encyclopedia Of Chemical Biology*.
- [4] **Reimhult, E., Zäch, M., Höök, F., Kasemo, B.A.** (2006). A multitechnique study of liposome adsorption on Au and lipid bilayer formation on SiO₂. *Langmuir*. 28;22(7):3313-9.
- [5] **Q-Sense.** Combined Qcm-D/Ellipsometry Setup For Real-Time Characterisation Of Thin Molecular Films, Application Note, QS 405-20-1.
- [6] **Q-Sense.** Quartz Crystal Microbalance with Dissipation (QCM-D), Technology Note, <http://www.q-sense.com/file/qcm-d-technology-note.pdf>, date retrieved 15.12.2011.
- [7] **Koolman, J., Roehm, K.** (2005). Color Atlas of Biochemistry, Second edition, p.50-51, *Thieme*.
- [8] **Avanti Polar Lipids.** Phosphatidylcholine, Avanti Polar Lipids Phospholipids, http://avantilipids.com/index.php?option=com_content&view=article&id=370&Itemid=256, date retrieved 10.12.2011.
- [9] **Gazit, E.** (2007). Plenty of Room for Biology at the Bottom: An Introduction to Bionanotechnology, p.40-41, *Imperial College*.
- [10] **Zhang, Z. and Guihua, H.** (2011). Micro- and Nano-Carrier Mediated Intra-Articular Drug Delivery Systems for the Treatment of Osteoarthritis, *School of Pharmaceutical Sciences*.
- [11] **Vasant, V. and Ranade, A.** (2004), Drug Delivery Systems, Second Edition, Chapter one, *CRC Press LLC*.
- [12] **Subhash, C. and Manju, Bas.** (n.d). Methods in Molecular Biology, Liposome Methods and Protocols, Volume 199, p.3-7, *Humana Press*.
- [13] **Andreas, W. and Karola, V.** (2011), Liposome Technology for Industrial Purposes, Corporation Journal of Drug Delivery, *Hindawi Publishing*.
- [14] **Marina, P., Marlene, L., José, L.** Liposomes As Drug Delivery Systems for the Treatment of TB: Liposome-based Drug Delivery Therapy, *Medscape*, http://www.medscape.com/viewarticle/752329_4, date retrieved 23.11.2011

- [15] **Avanti Polar Lipids.** Preparation of Liposomes, Avanti Polar Phospholipids, http://avantilipids.com/index.php?option=com_content&view=article&id=1384&Itemid=372, date retrieved 10.12.2011.
- [16] **Gregory, G.** (2007). Liposome Technology, Volume I Liposome Preparation and Related Techniques, p.60, Third Edition, *Informa Healthcare*.
- [17] **Kozubek A, Gubernator J, Przeworska E, Stasiuk M.** (2000). Liposomal drug delivery, a novel approach: PLARosomes, *Acta Biochimica Polonica*.
- [18] **Banerjee., R.** (2001). Liposomes Applications in Medicine, *Journal of Biomaterials Applications, J Biomater Appl*.
- [19] **Bakker-Woudenberg, I. A. J. M.** (1995). Delivery of antimicrobials to infected tissue macrophages. *Advanced Drug Delivery Reviews*, 17:5-20.
- [20] **Al-Jamal, T. and Kostas, K.** (2007). Construction of nanoscale multicompartiment liposomes for combinatory drug delivery. *International Journal of Pharmaceutics* 331 182–185. Pharmaceutical Nanotechnology.
- [21] **Al-Jamal, T. and Kostas, K.** (2007). Liposome–nanoparticle hybrids for multimodal diagnostic and therapeutic applications. *Nanomedicine* Vol. 2, No. 1, Pages 85-98.
- [22] **David S., G.** (2004). Bionanotechnology, Lessons from Nature, p.241-243, *Wiley-Liss*
- [23] **Reimhult, E., Kasemo, B., and Höök., F.** (2009). Rupture Pathway of Phosphatidylcholine Liposomes on Silicon Dioxide. *International Journal of Molecular Sciences*, 10, 1683-1696.
- [24] **Purrucker, O., Hillebrandt, H., Adlkofer, K. and Tanaka, M.** (2001). "Deposition of highly resistive lipid bilayer on silicon-silicon dioxide electrode and incorporation of gramicidin studied by ac impedance spectroscopy." *Electrochimica Acta*. 47. 791-798.
- [25] **Keller, C. A., Glasmaster, K., Zhdanov, V. P., Kasemo, B.** (2000). Formation of Supported Membranes from Vesicles. *Phys. Rev. Lett.* 84, 5443–5446.
- [26] **Cho, N.J., Cho, S.J., Cheong, K.H., Glenn, J.S., Frank, C.W.** (2007). Employing an Amphipathic Viral Peptide to Create a Lipid Bilayer on Au and TiO₂. *J. Am. Chem. Soc.*, 129 (33), pp 10050–10051.
- [27] **Jay T., G., Lara, K. M., and Carolyn R., B.** (2001). Control of Cell Adhesion and Growth with Micropatterned Supported Lipid Membranes. *Langmuir*, 17, 5129-5133.
- [28] **Svedhem, S., Dahlborg, D., Ekeröth, J., Kelly, J., Höök, F. and Gold, J.** (2003). In Situ Peptide-Modified Supported Lipid Bilayers for Controlled Cell Attachment. *Langmuir*, 19, 6730-6736.
- [29] **Gomide, A.B.,** QCM Analysis of Liposomes and Cells, http://www.ipeuropa.com/petra/es/actividades/petra2/becarios/Andreza_Barbosa/Project_Description_Andreza_Barbosa.pdf date retrieved 03.11.2011

- [30] **Basit, H. and Guerente, L.** (n.d). Initiation to QCM-D. Application notes.
- [31] **Kanazawa, K. and Nam-Joon C.** (2009). Quartz Crystal Microbalance as a Sensor to Characterize Macromolecular Assembly Dynamics, *Journal of Sensors* Volume 2009, *Hindawi Publishing*.
- [32] **Nicu, L., Leichle, T.** (2008). Biosensors and tools for surface functionalization from the macro to the nanoscale: The way forward. *J. App. Phys.*, 104, 111101 (1-16).
- [33] **Matthew A. and Victoria T.** (2007). A survey of the 2001 to 2005 quartz crystal microbalance biosensor literature: applications of acoustic physics to the analysis of biomolecular interactions. *Journal of Molecular Recognition*, Volume 20, Issue 3, pages 154–184
- [34] **Dixon, M.** (2008). Quartz Crystal Microbalance with Dissipation Monitoring: Enabling Real-Time Characterization of Biological Materials and Their Interactions. *J Biomol Tech.* 2008 July; 19(3): 151–158.
- [35] **Viitala, T.** (2005). Modeling the Mechanical Properties of Adsorbed/Deposited Layers at Air-Solid and Liquid-Solid Interfaces with the Dissipative KSV QCM-Z500, *KSV Instruments Ltd.*, Helsinki, pp. 1-33.
- [36] **Matthew A. and Victoria T.** (2007). A survey of the 2001 to 2005 quartz crystal microbalance biosensor literature: applications of acoustic physics to the analysis of biomolecular interactions. *Journal of Molecular Recognition*, Volume 20, Issue 3, pages 154–184
- [37] **Höök, F. and Rudh, M.** (2005). Quartz Crystal Microbalance in biomacromolecular recognition. [http://www.biotech-online.com/fileadmin/pdf/datasheet/quartz-crystal-microbalances-\(qcm\)-in-biomacromolecular-recognition.pdf](http://www.biotech-online.com/fileadmin/pdf/datasheet/quartz-crystal-microbalances-(qcm)-in-biomacromolecular-recognition.pdf) date retrieved 10.11.2011
- [38] **KSV.** (2004). QCM-Z500 Frequently Asked Questions, p. 1-3.
- [39] **Voinova, M. V., Rodahl, M., Johnson, M., Kasemo, B.** (1999). Viscoelastic acoustic response of layered polymer films at fluid-solid interfaces: Continuum mechanics approach, *Physica Scripta*, 59, 391-396.
- [40] **Van der Merwe, P.** (n.d). Surface plasmon resonance, users.path.ox.ac.uk/~vdmerwe/internal/spr.pdf, date retrieved 01.12.2011.
- [41] **Surface plasmon resonance.** (n.d). Terralab KSV SPR 200 Presentation.
- [42] **Miller, M. M. and Lazarides, A. A.** (2005). Sensitivity of metal nanoparticle surface plasmon resonance to the dielectric environment. *J. Phys. Chem. B*, 109, 21556-21565
- [43] **Willems, K. A. and Van Duyne, R. P.** (2007). Localized surface plasmon resonance spectroscopy and sensing, *Annu. Rev. Phys. Chem.*, 58, 267-297.
- [44] **Höpfner, M., Rothe, U. and Bendas, G.** (2008). Biosensor-Based Evaluation of Liposomal Behavior in the Target Binding Process, *Journal of Liposome research*, 18:71-82.

- [45] **Richter, R. P., Berat, R. and Brisson, A.** (2006). Formation of Solid Supported Lipid Bilayers: An Integrated View, *Langmuir*, 22, 3497-3505.
- [46] **Chang-Hai, W., Chi-Jen, L.** (2008). Optimizing the size and surface properties of polyethylene glycol (PEG)–gold nanoparticles by intense x-ray irradiation, *J. Phys. D: Appl. Phys.* 41
- [47] **Serro, A. P., Carapeto, A., Paiva, G.** (2011). Formation of an intact liposome layer adsorbed on oxidized gold confirmed by three complementary techniques: QCM-D, AFM and confocal fluorescence microscopy. *Surface and Interface Analysis*, 10.1002/sia.3820.
- [48] **Grönbeck, H., Curioni, A. and Andreoni, W.** (2000). Thiols and Disulfides on the Au(111) Surface: The Headgroup–Gold Interaction, *J. Am. Chem. Soc.*, 2000, 122 (16), pp 3839–3842.
- [49] **Reimhult, E., Hook, F. and Kasemo, B.** (2002). Intact Vesicle Adsorption and Supported Biomembrane Formation from Vesicles in Solution Influence of Surface Chemistry, Vesicle Size, Temperature, and Osmotic Pressure. *Langmuir* 2003, 19, 1681 1691.
- [50] **Knoll, W., Koper, I., Naumann, R., Sinner, E.** (2008). Tethered bimolecular lipid membranes—A novel model membrane platform. *Electrochimica Acta* 53 (2008) 6680–6689.
- [51] **Seantier, B. and Kasemo, B.** (2009). Influence of Mono- And Divalent Ions on the Formation of Supported Phospholipid Bilayers via Vesicle Adsorption. *Langmuir*, 25(10), 5767–5772.
- [52] **Porasso, R.D., López, C.** (2009). Study of the effect of Na⁺ and Ca²⁺ ion concentration on the structure of an asymmetric DPPC/DPPC + DPPS lipid bilayer by molecular dynamics simulation. *Colloids Surf B Biointerfaces*. Oct 1;73(1):42-50.

APPENDICES

APPENDIX A: Laboratory Equipments

APPENDIX B: Chemicals & Buffers

APPENDIX A

Laboratory Equipment

Pipettes (Eppendorf 10µl, 100 µl, 1000 µl, 2500 µl, 5000 µl)

pH meter (Hanna Instruments, HI 9124)

Magnetic stirrer (Cole-Parmer, Stable Temp)

Bath Sonicator (Transsonic TP 690)

Vortex (Heidolph, REAX top)

UV-Ozone System (Novascan, PSD Pro Series)

SPR (Reichert SR7000)

QCM-Z500 (KSV Instruments)

Optic Microscopy (Olympus)

Tubing (Tygon, SC0060; R3607)

Peristaltic pump

Filter Support (10mm Filter Supports, 610014 Avanti Polar)

PC Membranes (0.1µm Polycarbonate Membranes, 610005 Avanti Polar)

QCM slides (Q-Sense, Sweden)

SPR slides

Mini-Extruder (Avanti Polar Lipids/Hamilton Company, 610017)

Extruder membranes (Whatman, Nuclepore Track-Etch Membrane 0.1 µm, 800309)

APPENDIX B

Chemicals

DGPE (Avanti Polar Lipid, 870160)

PC (Sigma-Aldrich)

PBS (Phosphate buffered saline)

- 1.78 g $\text{Na}_2\text{HPO}_4 \cdot 2\text{H}_2\text{O}$
- 0.27 g KH_2PO_4
- 0.20 g KCl
- 8 g NaCl in 1 liter
- Adjust pH 7.4 with HCl or NaOH

Ethanol (Sigma, 32221-SL)

Isopropanol (Sigma, 24137)

Sodium Chloride

Potassium Chloride

Sodium Hydroxide

Hydrochloric Acid

Potassium Dihydrogenphosphate (KH_2PO_4)

Disodium Hydrogen Phosphate Dihydrate ($\text{Na}_2\text{HPO}_4 \cdot 2\text{H}_2\text{O}$)

Chloroform

SDS (sodium dodecyl sulfate)

CURRICULUM VITAE



Name Surname: Abdulhalim KILIÇ

Place and Date of Birth: Trabzon, 08.12.1984

Address: İTÜ D-2 Lojmanları No-91 Maslak/İstanbul

E-Mail: kilicabd@itu.edu.tr

B.Sc.: Molecular Biology and Genetics, İTÜ (2003-2008)

PUBLICATIONS/PRESENTATIONS ON THE THESIS

- **Kılıç, A.,** Kök, F.N. 2011: Supported Lipid Bilayers with Thiolated Lipids. *17th International Symposium on Biomedical Science and Technology (BIOMED 2011)*, November 23-25, 2011 Ankara, Turkey.